

Received March 30, 2021, accepted April 13, 2021, date of publication April 16, 2021, date of current version April 29, 2021.

Digital Object Identifier 10.1109/ACCESS.2021.3073821

# Identification of Solar Photovoltaic Model Parameters Using an Improved Gradient-Based Optimization Algorithm With Chaotic Drifts

M. PREMKUMAR<sup>1</sup>, (Member, IEEE), PRADEEP JANGIR<sup>1</sup>,  
C. RAMAKRISHNAN<sup>2</sup>, (Member, IEEE), G. NALINIPRIYA<sup>3</sup>, (Member, IEEE),  
HASSAN HAES ALHELLOU<sup>4</sup>, (Senior Member, IEEE),  
AND B. SANTHOSH KUMAR<sup>5</sup>, (Senior Member, IEEE)

<sup>1</sup>GMR Institute of Technology, Rajam 532127, India

<sup>2</sup>Rajasthan Rajya Vidyalaya Prasaran Nigam Limited, Sikar 332025, India

<sup>3</sup>SNS College of Technology, Coimbatore 641035, India

<sup>4</sup>Saveetha Engineering College, Chennai 602105, India

<sup>5</sup>School of Electrical and Electronic Engineering, University College Dublin, Dublin 4, D04 V1W8 Ireland

<sup>6</sup>Guru Nanak Institute of Technology, Hyderabad 501506, India

Corresponding authors: Hassan Haes Alhelou (alhelou@ieee.org) and M. Premkumar (mprem.me@gmail.com)

The work of Hassan Haes Alhelou was supported in part by the Science Foundation Ireland (SFI) through the SFI Strategic Partnership Programme under Grant SFI/15/SPP/E3125, and in part by the University College Dublin (UCD) Energy Institute.

**ABSTRACT** When discussing the commercial applications of photovoltaic (PV) systems, one of the most critical problems is to estimate the efficiency of a PV system because current (I) – voltage (V) and power (P) – voltage (V) characteristics are highly non-linear. It should be noted that most of the manufacturer's datasheets do not have complete information on the electrical equivalent parameters of PV systems that are necessary for simulating an effective PV module. Compared to conventional approaches, computational optimization and global research strategies are more acceptable as an effective alternative to parameter estimation of solar PV modules. Recently, a Gradient-based optimizer (GBO) is reported to solve the engineering design optimization problems. However, the basic GBO algorithm is stuck in local optima when handling complex non-linear problems. In this sense, this paper presents a new optimization technique called the Chaotic-GBO (CGBO) algorithm to derive the parameters of PV modules while offering precise I-V and P-V curves. To this end, the CGBO algorithm is based on a chaotic generator to obtain the PV parameters combined with the GBO algorithm. There are five case studies considered to validate the performance of the proposed CGBO algorithm. A quantitative and qualitative performance evaluation reveals that the proposed CGBO algorithm has improved results than other state-of-the-art algorithms in terms of accuracy and robustness when obtaining PV parameters. The average RMSE values and runtime of five case studies are equal to 9.8427E-04, 2.3700E-04, 2.4251E-03, 4.3524E-03 and 1.8349E-03, and 18.44, 17.78, 18.18, 18.28 and 17.97, respectively. The results proved the superiority of the proposed CGBO algorithm over the different selected algorithms. For future research, this study will be backed up with external support at <https://premkumarmanoharan.wixsite.com/mysite>.

**INDEX TERMS** Chaotic-gradient-based optimizer (CGBO), chaotic generator, gradient-based optimizer (GBO), parameter estimation, photovoltaics.

## I. INTRODUCTION

Solar power sources are viable and promising alternatives to diverse forms of renewable energy sources [1]. Indeed,

The associate editor coordinating the review of this manuscript and approving it for publication was Huaqing Li<sup>1</sup>.

the availability, sustainability, and inexhaustibility of solar energy have enabled it one of the most vital forms of renewable energy in recent decades. Their incorporation into classical power systems with high penetration is equipped to enhance the output in terms of steady-state and dynamic performance [2]. A detailed model that specifically defines the

behavior of photovoltaic panels for various industrial applications (array fault detection, power controller and controller configuration, maximum power point tracking techniques, grid integration, etc.) is quite essential and thus increases the overall performance of PV systems [3]. Accurate modeling of PV modules is therefore required to reflect their characteristics for further study. As per the scientific studies relating to the field of PV system modeling, a single-diode equivalent model (SDeM) [4], double-diode equivalent model (DDeM) [5], and three-diode equivalent model (TDeM) [6] can be used to represent the PV cell or module. The cell or module parameters that should be estimated for each PV model are photocurrent  $I_p$ , diode ideality factor  $n$ , series resistance  $R_s$ , shunt resistance  $R_p$ , and diode-reverse saturation current  $I_{sd}$ . For the SDeM, DDeM, and TDeM, respectively, the number of unknown parameters is five, seven, and nine [7].

Numerous techniques have been reported to estimate the parameters of the various models based on the experimental samples or the datasheet information. The methods are classified as follows: numerical methods, analytical methods, and heuristics methods [8]–[10]. In the literature, numerical methods are commonly used; such techniques use numerical solutions to identify a network of a few non-linear PV model-related equations [11], [12]. The analytical techniques use a sequence of generalizations and assumptions to evaluate the model parameters to obtain explicit equations, usually depending on multiple critical points on the I-V characteristics [9], [10], [13]. The authors [14] presented an analytical method to extract the five parameters of the SDeM, and the authors also investigated the performance of the parameters on open-circuit voltage, short-circuit current, and maximum power point. Biological events typically inspire the heuristic techniques to approximate the parameters of the model to solve specific weaknesses and challenges of the first two techniques, such as differentiability, convexity, and extreme sensitivity to the initial parameter values. It should be stated that, because of its precision, reliability, and unregulated by the initial values, a heuristic approach may have good outcomes than the other methods [7], [15]–[17].

In recent years, several researchers have made a great deal of effort to use algorithm-based on metaheuristics to solve such problems. These structures are influenced by natural events, such as swarming activities, mechanisms focused on nature, and physics. Genetic algorithm (GA) [18], [19], particle swarm optimization [20]–[22], enhanced leader particle swarm optimization algorithm (PSO) [23], niche particle swarm optimization in parallel computing algorithm [24], several versions of differential evolution (DE) [25]–[28], penalty-based DE algorithm [29], sunflower optimizer [30], grey wolf optimizer (GWO) [31], whale optimizer algorithm (WOA) [32], harris-hawk optimizer (HHO) [33], improved salp swarm algorithm (ISSA) [34], several version of JAYA algorithm [35], multiple learning backtracking search algorithm [36], coyote optimization algorithm [37], teaching-learning-based optimization and its various ver-

sions [38]–[42], political optimizer (PO) [4], evolutionary shuffled frog leaping algorithm [43], slime-mould optimizer (SMO) [44], [45], marine predator algorithm (MPA) [46], equilibrium optimizer (EO) [47], ions motion optimization (IMO) [48], improved PSO (IPSO) [49], Forensic-based investigation algorithm [50], and improved learning-search algorithm [51] are among good heuristic-based structures. Some studies have endeavored to hybridize a few of these strategies to boost their performance, such as hybrid grey wolf optimizer with cuckoo search algorithm [52], hybrid firefly with pattern search algorithms [53], hybrid grey wolf optimizer with particle swarm algorithm [54], hybrid WO with DE algorithm [26], hybrid GA with simulated annealing algorithm [18], etc. Based on the literature study, the comparison between few well-known algorithms based on the control parameters is presented in Appendix (Refer to Table 25). It is important to note that the random number generator is the basis of all the algorithms and approaches mentioned earlier. It can be concluded that each method has its own pros and cons, and therefore all complicated problems cannot be solved by any learning algorithm. Furthermore, there is still no clear answer, or it is tough to decide that optimization approach A would be most appropriate for problem B of many features such as modality, control variables, convexity, degree of non-linearity, separability, etc., as per the no-free-lunch (NFL) theorem [55]. In such pursuits, the effort continues until such an answer is obtained.

On the other side, numerous early efforts have also shown that several useful optimization techniques, the introduction of chaos theory can lead to a massive enhancement compared to its original variant. As a piece of evidence, chaos theory has been evaluated to produce random sequences because chaotic patterns are simultaneously deterministic and uncontrollable and can therefore be seen as a random number generator [56]. Several chaos generators, such as Sprott, Linz-Sprott, Chua, Rossler, and Lorenz types, have been intended to support data encryption and parallel computing application areas. Several other productive features of chaos theory make them perfect for many engineering applications, such as power systems, communication systems, image segmentation, feature selection, mechanical design systems, encrypted systems, and so on. Moreover, to obtain the parameters of solar PV models, published studies have integrated chaotic patterns and various forms of optimization techniques. Artificial bee colony with the chaotic pattern is employed in [57]. The authors introduced a logistic-chaotic map in [58] to solve updating process of the JAYA algorithm. The authors of [35] introduced chaotic adaptive weight factors with the JAYA algorithm to estimate the parameters of various PV models. In [59], different PV model parameters are obtained under multiple climatic conditions based on the fractional chaotic ensemble PSO. The static and dynamic fractional-order parameters of PV models are estimated in [60] via chaotic and comprehensive learning PSO. The authors of [61] applied four chaotic maps during the parameter identification of SDeM and DDeM to enhance the basic WO's productivity. A new variant of the HHO algorithm

is based on chaotic drifts to obtain the unknown parameters of PV cells and modules modeled via SDeM and DDeM [62]. Another variant of HHO is combining crisscross algorithm features and the Nelder-mead simplex method to improve the solution accuracy [63].

While various optimization techniques have been successfully introduced to the extraction of PV module parameters, it is still essential to implement a new algorithm to achieve greater precision and, as a result, to enhance the overall efficiency of various industrial Photovoltaic systems, mainly when there is a wide selection of errors such as 10e-4. Since the NFL theorem suggests that no algorithm can provide appropriate results and best results in all optimization problems, these optimization techniques, and their variants have been developed many times [55]. Despite the various apparent methods referred to above to identify the ambiguous parameters of PV models with acceptable performance, and yet again, there is still space for progress to define the PV models specifically.

The key objective of this paper is indeed to obtain the parameters of the PV models of SDeM and DDeM by leveraging the significance of combining a chaos map with the basic gradient-based optimizer (GBO) [64]. Newton's equations inspire the GBO algorithm, and the exploration and exploitation balance is maintained by the local escaping operator and gradient search rule. In the updating stage of the GBO algorithm, the suggested technique exploits sensitivity to the initial conditions of systems to check for a new solution and thereby achieve a desirable improvement in the objective values, i.e., Root-Mean-Square-Error (RMSE) values [65]. The basic version of the GBO algorithm gets trapped by the local optima when handling non-linear multimodal objective functions. In addition, due to the randomness, the convergence speed is low. The basic version needs to be modified to improve the solution accuracy as well as convergence speed. Therefore, a chaotic drift is introduced along with the GBO algorithm to improve the solution accuracy and convergence speed. The development of the basic GBO algorithm by changing the parameters that govern the exploration and exploitation stages is one of the key contributions of this paper, thereby reducing its search space to achieve appropriate balance using the chaotic tent map. The experimental sample of PV SDeM and DDeM is used to assess the proposed chaotic-based GBO (CGBO) algorithm. The findings of the suggested algorithm are contrasted to that of other state-of-the-art algorithms. The findings demonstrated that the CGBO is more efficient and superior to different algorithms. A review of results reveals that the GBO algorithm with a chaotic-based search sequence outperforms several modern well-known optimization techniques in terms of reliability and precision when extracting the parameters of various PV models. The highlights of the paper are as follows.

- A new version of the GBO algorithm called the CGBO algorithm is introduced to solve the parameter estimation problem of various PV models.

- The chaotic tent map replaces the randomness of the GBO algorithm and helps to increase the solution accuracy and convergence speed.
- The proposed CGBO is verified on various PV models, such as SDeM, DDeM, and PV models, and compared with different state-of-the-art algorithms.
- The performance of CGBO is assessed in terms of the convergence speed and RMSE values in comparison to different optimizers.
- The CGBO algorithm is also validated under different operating conditions and demonstrated high accuracy in the experimental and optimized values.

The structure of the paper is planned as follows. Section 2 explains the mathematical modeling of various PV models; in addition, the problem formulation is also presented. Section 3 discusses the formulation of the proposed CGBO algorithm, and Section 4 discusses the experimental findings in detail. Section 5 delivers the concluding remarks and future research directions.

## II. MODELING OF PHOTOVOLTAIC MODELS AND PROBLEM FORMULATION

The SDeM and DDeM are considered to be effective PV models as per the detailed study from various literature [66]–[69]. Therefore, this section of the paper discusses the mathematical modeling of different photovoltaic models. In addition, the objective function formulation is also discussed in this section.

### A. MATHEMATICAL MODELLING

Various methodologies were used in the literature for photovoltaic cell/module simulation. In a recent study, the equivalent circuit of the cell/module is usually used among all the current approaches. The key benefit of using this model is the simplicity with which it can be implemented using the MATLAB software tool. The preceding Shockley equation defines the PV cell's I-V characteristic.

$$I_d = I_{sd} \left[ \exp \left( \frac{q \times V_d}{aKT} \right) \right] \quad (1)$$

where  $I_d$  denotes the diode current,  $I_{sd}$  denotes reverse saturation current of the diode,  $q (= 1.60217646 \times 10^{-19} \text{ C})$  denotes electron charge,  $k (= 1.380653 \times 10^{-23} \text{ J/K})$  denotes Boltzmann's constant,  $a$  denotes diode ideality factor,  $T$  denotes temperature in K, and  $V_d$  denotes the diode voltage. When the PN junction gains an electron from the sunlight, a set of electron-holes is formed in the presence of irradiation. This produces a potential gap around the junction. At which point, charge carriers continue to pass via the external circuit, resulting in an electrical current  $I_p$ , which is referred to as the photocurrent. As a result, the ideal model of the cell has a current generator connected in parallel with the diode. The output current  $I$  of the PV cell for the new model is given in Eq. 2.

$$I = I_p - I_{sd} \left[ \exp \left( \frac{q \times V_d}{aKT} \right) \right] \quad (2)$$

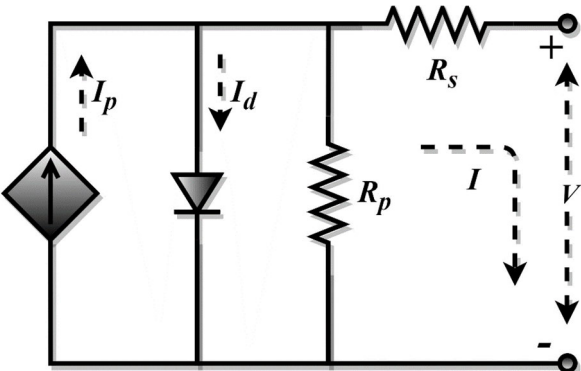


FIGURE 1. SDeM of the PV cell.

Since the PV cell supplies ohmic losses, the model has to consider the effect of series resistance  $R_s$ . Therefore, the output current of the PV cell by considering the impact of  $R_s$  is given in Eq. 3.

$$I = I_p - I_{sd} \left[ \exp \left( \frac{q(V + IR_s)}{aKT} \right) - 1 \right] \quad (3)$$

where  $V$  denotes the output voltage. However, the model discussed above is not accurate because the model does not consider the effect of the leakage current of the cell. Therefore, the impact of shunt resistance needs to be considered when describing the actual model of the PV cell. By combining all the elements and parameters, the PV cell is modeled initially as SDeM. The SDeM is a simple and most preferred PV model for the analysis. The SDeM is shown in Fig. 1. Furthermore, now, the total output current of the PV cell is given in Eq. 4.

$$I = I_p - I_{sd} \left[ \exp \left( \frac{q(V + IR_s)}{aKT} \right) - 1 \right] - \frac{(V + IR_s)}{R_p} \quad (4)$$

From Eq. 4, it is observed that the PV SDeM is defined by five uncertain variables, which are presented in Eq. 5.

$$\xi = \{I_p, I_{sd}, a, R_s, R_p\} \quad (5)$$

Recombination is an important failure in an actual cell that cannot be adequately modeled with one diode. As a result, a second diode is connected to the SDeM to correct for the impact of composite current failure. Fig. 2 displays the circuit of the DDeM. As a consequence, the I-V characteristic is given in Eq. 6.

$$I = I_p - I_{sd1} \left[ \exp \left( \frac{q(V + IR_s)}{a_1 KT} \right) - 1 \right] - I_{sd2} \left[ \exp \left( \frac{q(V + IR_s)}{a_2 KT} \right) - 1 \right] - \frac{(V + IR_s)}{R_p} \quad (6)$$

where  $I_{sd1}$  and  $I_{sd2}$  denote the saturation and diffusion currents, respectively, and  $a_1$  and  $a_2$  refer to the recombination and diffusion diode-ideality factors, respectively.

From Eq. 6, it is observed that the PV DDeM is defined by seven uncertain variables, which are presented in Eq. 7.

$$\xi = \{I_p, I_{sd1}, I_{sd2}, a_1, a_2, R_s, R_p\} \quad (7)$$

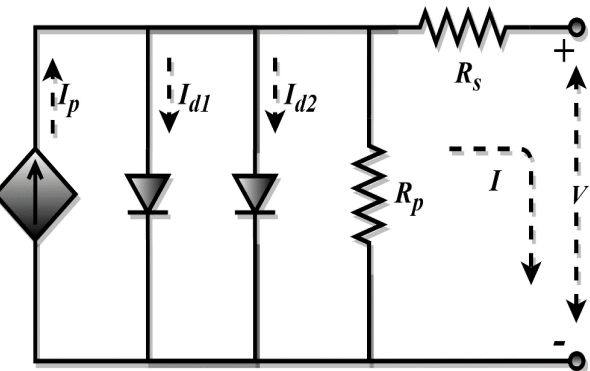


FIGURE 2. DDeM of the PV cell.

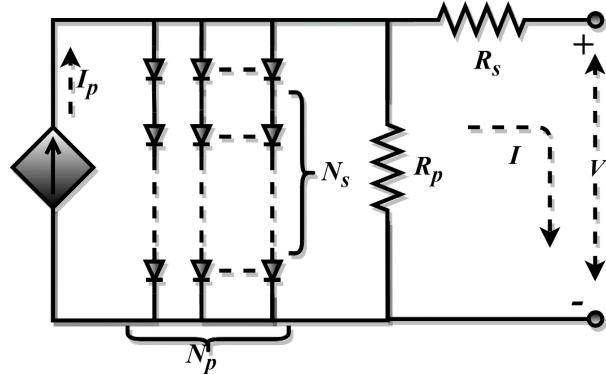


FIGURE 3. Equivalent circuit of the PV module.

The mathematical equations of the SDeM and DDeM can be interpreted as follows in the context of a PV module composed of  $N_p$  cells parallel-connected and  $N_s$  cells series-connected. The equivalent circuit of the PV module is illustrated in Fig. 3.

$$I = N_p I_p - N_p I_{sd} \left[ \exp \left( \frac{q(V + (N_s/N_p) IR_s)}{aN_s KT} \right) - 1 \right] - \frac{(V + (N_s/N_p) IR_s)}{(N_s N_p) R_p} \quad (8)$$

$$I = N_p I_p - N_p I_{sd1} \left[ \exp \left( \frac{q(V + (N_s/N_p) IR_s)}{a_1 N_s KT} \right) - 1 \right] - I_{sd2} \left[ \exp \left( \frac{q(V + (N_s/N_p) IR_s)}{a_2 N_s KT} \right) - 1 \right] - \frac{(V + (N_s/N_p) IR_s)}{(N_s/N_p) R_p} \quad (9)$$

Both SDeM and DDeM of the PV cell/module have undefined variables that can be calculated numerically, analytically, or using optimization techniques.

## B. OBJECTIVE FUNCTION FORMULATION

The undefined SDeM and DDeM parameters of Eqs. 5 and 7 must be calculated for both cell and module. The uncertain variables are being used as a decision variable in the optimization procedure. The root mean square error (RMSE) between the optimized and experimental samples is being used as an objective function. Integral absolute error (IAE), relative error (RE), and RMSE are determined using the following expressions.

$$IAE_i = |I_{act} - I_{est}| \quad (10)$$

$$RE = \frac{I_{act} - I_{est}}{I_{act}} \quad (11)$$

$$IAE_p = |P_{act} - P_{est}| \quad (12)$$

$$RMSE = \sqrt{\frac{1}{N} \sum_{j=1}^N (I_i - I_{(V_i, \xi)})^2} \quad (13)$$

where  $I_{act}$  defines the experimental current,  $I_{est}$  refers to the optimized current,  $IAE_i$  denotes integral absolute error based on current,  $IAE_p$  denotes integral absolute error based on power,  $N$  refers to the number of experimental voltage and current samples ( $V_i$ ,  $I_i$ ), and  $I_{(V_i, \xi)}$  refers to the optimized value as a function of the undefined variables  $\xi$ , which are defined by Eqs. 5 and 7.

The objective function or fitness function is a function that evaluates the degree of correlation between the configuration of variables that characterize the model and experimental results. The objective function in this analysis observes the variation between experimental and predicted values. The parameter estimation aims to reduce the error between the expected parameters and the experimental parameter, which is represented as follows.

$$\text{Min (RMSE)} = \text{Min} \left( \sqrt{\frac{1}{N} \sum_{j=1}^N (I_i - I_{(V_i, \xi)})^2} \right) \quad (14)$$

When the precise model parameters are obtained, the objective function could ideally be zero. Since the frameworks are so well-defined and no data on the exact predictions of variables is available, the degree of coordination depends mainly on the experimental sample. Consequently, every reduction in the RMSE value is crucial, meaning that the developer's knowledge of the real parameter estimates has increased.

## III. PROPOSED CHAOTIC WITH GRADIENT-BASED OPTIMIZER (CGBO) ALGORITHM

This section of the paper describes the basic variant of the GBO algorithm. Then, the process of extending the GBO to an improved CGBO is presented, and how CGBO is applied to the parameter estimation problem is also explained.

## A. ORIGINAL GRADIENT-BASED OPTIMIZER (GBO) ALGORITHM

Many circumstances, such as optimal power flow, economic load dispatch, solar PV parameter estimation, controller tuning, economic emission dispatch, could pose challenging tasks, as well as various types of objectives, such as multi-objective, many-objective, large-scale objectives, and fuzzy optimization. Regardless of whether the problem is a challenge or not, the real-time application requires a timely solution. In general, algorithms can be divided into the following categories based on behaviors: the algorithm that uses exact information, gradient, and sub-gradient information and slope, and the algorithm that use anticipated predicted solutions. Most of these methodologies could have a successful result, while others have unpredictable effectiveness. The GBO algorithm is a new population and gradient-based metaheuristic optimization algorithm [64]. To explore the whole search space, it primarily employs a set of vectors and two operators.

### 1) INITIALIZATION PHASE

In GBO, the variable  $\alpha$  is considered to be a transformative variable that transforms from the exploration phase to the exploitation phase. The probability rate is the only control variable in the GBO algorithm. The population size  $N$  and the number of iterations are chosen based on the problem complexity. The individual in the population is referred as a vector, and thus GBO comprises  $N$  vectors in  $D$ -dimensional search space. The vector is expressed as follows.

$$\begin{aligned} X_{d,x} &= [X_{1,x}, X_{2,x}, \dots, X_{D,x}] \\ x &= 1, 2, \dots, N \\ d &= 1, 2, \dots, D \end{aligned} \quad (15)$$

The initial position of the vector individuals is generated randomly in  $D$ -dimensional search space. The same has been expressed as follows.

$$X_x = X_l + rand(0, 1) \times (X_u - X_l) \quad (16)$$

where  $rand$  denotes random number between  $[0, 1]$ , and  $X_u$  and  $X_l$  are the upper and lower boundaries of the decision variables  $X$ .

### 2) GRADIENT SEARCH RULE (GSR)

The vector movements are controlled in the gradient search rule (GSR), which obtains quality solutions by improving the exploration in the promising area. The GSR helps GBO to strengthen its exploration phase and the convergence rate. The GSR permits the GBO to fine-tune for the random movements to avoid premature convergence and improve the exploration ability. The convergence rate is simplified by means of the direction of movement (DM). So, the current position of the population is updated using Eq. 14.

$$X_1^m = x_x^m + DM - GSR \quad (17)$$

$$GSR = \rho_1 \times randn \times \frac{2\Delta x \times x_x^m}{(x_w - x_b + \epsilon)} \quad (18)$$

$$\text{DM} = \rho_2 \times \text{rand} \times (x_b - x_x^m) \quad (19)$$

The vector updates its position by Eq. 17, and the updated vector is referred to as  $X1_x^m$ . The terms  $m$  denotes the iteration and  $\rho_1$  denotes important control variables to balance exploration and exploitation. The variable  $\varepsilon$  is within the range of  $[0, 0.1]$ . The best and the worst solutions are denoted as  $x_b$  and  $x_w$ , respectively.

$$\rho_1 = 2 \times \alpha \times \text{rand} - \alpha \quad (20)$$

$$\alpha = \left| \beta \times \sin \left( \frac{3\pi}{2} + \sin \left( \frac{3\pi}{2} \times \beta \right) \right) \right| \quad (21)$$

$$\beta = (\beta_{max} - \beta_{min}) \times \left( 1 - \left( \frac{m}{m_{max}} \right)^3 \right)^2 + \beta_{min} \quad (22)$$

where  $m_{max}$  denotes the maximum number of iterations,  $\text{randn}$  denotes uniformly distributed random number,  $\beta_{max} = 1.2$  and,  $\beta_{min} = 0.2$ . The parameter  $\delta$  verifies that the  $\Delta x$  is altered during every iteration or no, and  $\Delta x$  denotes the difference between the current position and the randomly chosen position.

$$\Delta x = |\text{step}| \times \text{rand} (1 : N_p) \quad (23)$$

$$\text{step} = \frac{\delta + (x_b - x_{r1}^m)}{2} \quad (24)$$

$$\delta = \text{rand} \times 2 \times \left| \frac{x_{r1}^m + x_{r2}^m + x_{r3}^m + x_{r4}^m}{4} - x_x^m \right| \quad (25)$$

where  $r_1, r_2, r_3$ , and  $r_4(r_1 \neq r_2 \neq r_3 \neq r_4 \neq n)$  are integers, and the values are chosen randomly between  $[1, D]$ . The step size  $\text{step}$  is obtained by  $x_b$  and  $x_{r1}^m$ . The additional random variable which helps during the exploration stage is denoted as  $\rho_2$  and it is expressed as follows.

$$\rho_2 = 2 \times \alpha \times \text{rand} - \alpha \quad (26)$$

And now, Eq. 17 can be rewritten as follows.

$$\begin{aligned} X1_x^m &= x_x^m - \rho_1 \times \text{randn} \times \frac{2\Delta x \times x_x^m}{x} (\varepsilon + yp_x^m - yq_x^m) \\ &\quad + \rho_2 \times \text{rand} \times (x_b - x_x^m) \end{aligned} \quad (27)$$

A new population vector  $X2_x^m$  is expressed in Eq. 28.

$$\begin{aligned} X2_x^m &= x_b - \rho_1 \times \text{randn} \times \frac{2\Delta x \times x_x^m}{(\varepsilon + yp_x^m - yq_x^m)} \\ &\quad + \rho_2 \times \text{rand} \times (x_{r1}^m - x_{r2}^m) \end{aligned} \quad (28)$$

$$yq_x = \text{rand} \times \left( \frac{[z_{x+1} + x_x]}{2} - \Delta x \times \text{rand} \right) \quad (29)$$

$$yp_x = \text{rand} \times \left( \frac{[z_{x+1} + x_x]}{2} + \Delta x \times \text{rand} \right) \quad (30)$$

The search direction technique improves the exploitation stage. The searching process is initiated as per Eq. 28 for the local search alone, and Eq. 27 is used for global search alone. Thus, both search processes are required to improve the exploration and exploitation phases. Based on the above-all

**TABLE 1.** Various chaotic maps.

Map Type	Chaotic Behavior	Range
Circle	$x_{i+1} = \text{mod} \left( x_i + b - \left( \frac{a}{2\pi} \right) \sin(2\pi x_k, 1) \right)$ $a = 0.5, b = 0.2$	
Sinusoidal	$x_{i+1} = ax^2 \sin(\pi x_i), a = 2.3$	
Sine	$x_{i+1} = \frac{a}{4} \sin(\pi x_i), a = 4$	
Gauss/mouse	$x_{i+1} = \begin{cases} 1, & x_i = 0 \\ \frac{1}{\text{mod}(x_i, 1)}, & \text{Otherwise} \end{cases}$	
Singer	$x_{i+1} = \mu(7.86x_i - 23.31x_i^2 + 28.75x_i^3 - 13.302875x_i^4), \mu = 1.07$	
Iterative	$x_{i+1} = \frac{\sin(a\pi)}{x_i}, a = 0.7$	
Tent	$x_{i+1} = \begin{cases} \frac{x_i}{0.7}, & x_i < 0.7 \\ \frac{10}{3}(1 - x_i), & x_i \geq 0.7 \end{cases}$	[0,1]
Piecewise	$x_{i+1} = \begin{cases} \frac{x_i}{p}, & 0 \leq x_i < p \\ \frac{x_i - p}{0.5 - p}, & p \leq x_i < 0.5 \\ \frac{1 - p - x_i}{0.5 - p}, & 0.5 \leq x_i < 1 - p \\ \frac{1 - x_i}{p}, & 1 - p \leq x_i < 1 \end{cases}, p = 0.4$	
Logistic	$x_{i+1} = ax_i(1 - x_i), a = 4$	
Chebyshev	$x_{i+1} = \cos(i \cos^{-1}(x_i))$	[-1,1]

discussions, the solution  $x_x^{m+1}$  is updated during the next iteration as follows.

$$X3_x^m = X_x^m - \rho_1 \times (X2_x^m - X1_x^m) \quad (31)$$

$$\begin{aligned} x_x^{m+1} &= r_a \times (r_b \times X1_x^m + (1 - r_b) \times X2_x^m) \\ &\quad + (1 - r_a) \times X3_x^m \end{aligned} \quad (32)$$

where  $r_a$  and  $r_b$  denote random numbers between [0,1].

### 3) LOCAL ESCAPING OPERATOR (LEO)

The LEO is a very useful operator in GBO to solve complex optimization problems. By utilizing several possible solutions, The LEO generates a quality solution  $X_{LEO}^m$  using solutions, such as  $X1_x^m, X2_x^m, x_{r1}^m, x_{r2}^m, x_b$ , and  $x_k^m$ . Eq. 33 is used to produce  $X_{LEO}^m$ .

```

if rand < P_r
    if rand < 0.5
        X_{LEO}^m = X_x^{m+1} + a \times (a_1 \times x_b - a_2 \times x_k^m)
        + b \times \rho_1 \times (a_3 \times (X2_x^m - X1_x^m) + a_2 \times (x_{r1}^m - x_{r2}^m)) / 2
        X_x^{m+1} = X_{LEO}^m
    else
        X_{LEO}^m = x_b + a \times (a_1 \times x_b - a_2 \times x_k^m) + b \times \rho_1
        \times (a_3 \times (X2_x^m - X1_x^m) + a_2 \times (x_{r1}^m - x_{r2}^m)) / 2
    end
end

```

(33)

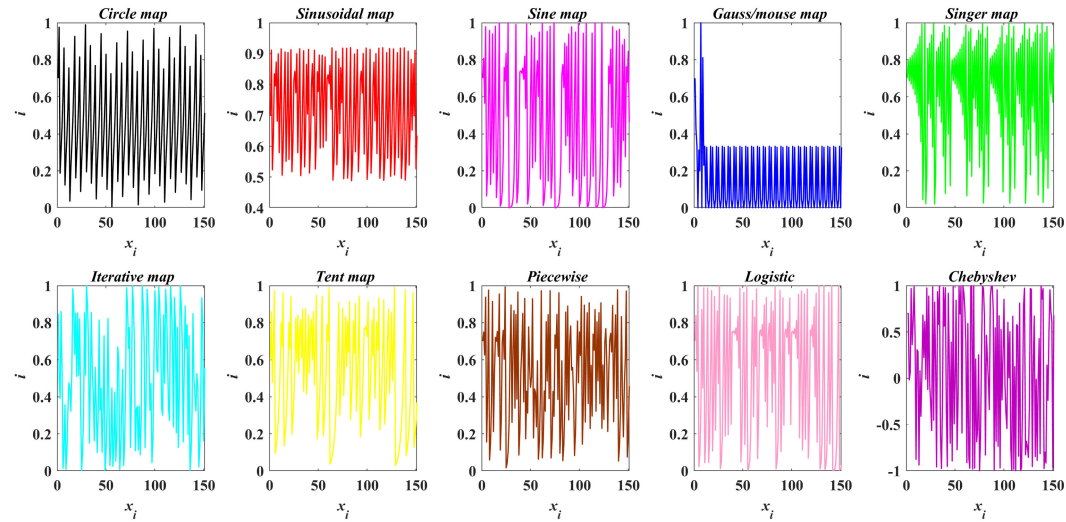


**FIGURE 4.** Various chaos maps number distribution.

where  $b$  referred to as a normally distributed random number with a mean of 0 and standard deviation of 1,  $a$  referred to as a uniform random number between  $[-1, 1]$ , and  $P_r$  denotes the probability rate. The random numbers, such as  $a_1$ ,  $a_2$ , and  $a_3$  are expressed as follows.

$$a_1 = Z_1 \times \text{rand} \times 2 + (1 - Z_1) \quad (34)$$

$$a_2 = a_3 = Z_1 \times \text{rand} + (1 - Z_1) \quad (35)$$

The value of  $Z_1$  is 0 or 1. The solution  $x_k^m$  is calculated using Eq. 33.

$$x_k^m = \begin{cases} x_{\text{rand}}, & \text{if } u_2 < 0.5 \\ x_p^m, & \text{otherwise} \end{cases} \quad (36)$$

$$x_{\text{rand}} = X_l + \text{rand} \times (X_u - X_l) \quad (37)$$

where  $x_{\text{rand}}$  denotes the new solution,  $x_p^m$  denotes the solution of random population, and  $u_2$  denotes a random number between  $[0,1]$ . Thus, Eq. 36 is revised as follows.

$$x_k^m = Z_2 \times x_p^m + (1 - Z_2) \times x_{\text{rand}} \quad (38)$$

The value of  $Z_1$  is 0 or 1 based on the value of  $u_2$ . The pseudocode of the GBO is presented in **Algorithm 1**.

### B. GRADIENT-BASED OPTIMIZER WITH CHAOTIC DRIFT

In the current decade, there has been a trend to use chaotic behaviors to replace the heuristic algorithm's randomness in order to capture the strongest stochastic and statistical properties of chaotic randomization. Various chaotic maps are listed in Table 1, and the respective map distribution is illustrated in Fig. 4.

All the chaos maps are started with an initial value of 0.7. The update equation of GBO is shown in Eq. 32, in which  $r_a$  and  $r_b$  are the random numbers between 0 and 1. The update equation of the GBO is modified by replacing the random numbers  $r_a$  and  $r_b$  with the chaos maps listed in Table 1 to improve the solution accuracy and convergence speed of the basic version of the GBO algorithm. The modified update

---

### Algorithm 1 Pseudocode of the GBO Algorithm

---

#### Step 1: Initialization Phase

Assign values for  $P_r$ ,  $m_{\max}$ , and  $\varepsilon$  and asses the fitness function value,  $f(X_x)$ ,  $x = 1, 2, \dots, N$ .  
Specify  $x_w^m$  and  $x_b^m$ .

#### Step 2: Main Loop

```

while ( $m < m_{\max}$ )
  for  $x = 1:N$ 
    Randomly choose  $r_1 \neq r_2 \neq$ 
     $r_3 \neq r_4 \neq n$  in the range of
     $[1, nN]$  Obtain the solution
     $x_x^{m+1}$ 
    using Eq. 32
  end for
  Local Escaping Operator (LEO)
  if  $\text{rand} < P_r$ 
    Obtain the solution
     $x_{LEO}^m$  using Eq. 33
     $X_x^{m+1} = x_{LEO}^m$ 
  end if
  Update the solutions,  $x_w^m$  and  $x_b^m$ 
  end for
end while

```

**Return the best solution**

---

equation of the GBO algorithm is presented in Eq. 39, in which  $C_a$  and  $C_b$  are chaotic numbers generated by various chaos maps. After many trials, it is found that the random number generated by the tent map is superior to all other maps listed in Table 1. Therefore, in this paper, it is decided to select a tent map to generate  $C_a$  and  $C_b$ .

$$x_x^{m+1} = C_a \times (r_b \times X_x^m + (1 - C_b) \times X_x^{m+1}) + (1 - C_a) \times X_x^m \quad (39)$$

**TABLE 2.** Parameter settings of all selected algorithms.

Algorithm	Control Parameters	Value
GBO	$N$	30 (SDeM) 50 (DDeM & Others)
	$m_{max}$	1000
	$P_r$	0.5
CGBO	$\varepsilon$	0.005
	$N$	30 (SDeM) 50 (DDeM & Others)
	$m_{max}$	1000
IMO	$P_r$	0.5
	$\varepsilon$	0.005
	$N$	30 (SDeM) 50 (DDeM & Others)
EO	$m_{max}$	1000
	$N$	30 (SDeM) 50 (DDeM & Others)
	$m_{max}$	1000
WOA	$a_1, a_2$ , and $RP$	2, 1, and 0.5, respectively
	$N$	30 (SDeM) 50 (DDeM & Others)
	$m_{max}$	1000
MPA	$N$	30 (SDeM) 50 (DDeM & Others)
	$m_{max}$	1000
	$FADS$	0.5
IPSO	$p$	0.5
	$N$	30 (SDeM) 50 (DDeM & Others)
	$m_{max}$	1000
PSO	$w_{Max}$ and $w_{Min}$	0.9 and 0.4
	$c_1$ and $c_2$	2
	$N$	30 (SDeM) 50 (DDeM & Others)
PSO	$m_{max}$	1000
	$w_{Max}$ and $w_{Min}$	0.9 and 0.6
	$c_1$ and $c_2$	2

The chaotic tent sequence is presented in Eq. 40.

$$C_{m+1} = \begin{cases} \frac{C_m}{0.7}, & C_m < 0.7 \\ \frac{10}{3}(1 - C_m), & C_m \geq 0.7 \end{cases} \quad (40)$$

where  $C_m$  denotes the random number of  $m^{\text{th}}$  iteration and  $C_1$  is generated randomly between [0, 1], and its initial value is selected as 0.6. Fig. 5 illustrates the overall flowchart of the proposed CGBO algorithm.

#### IV. SIMULATION RESULTS AND DISCUSSIONS

This section of the paper discusses the experimental study of the proposed CGBO algorithm. Therefore, the performance of CGBO is validated on different PV models of various PV cells and PV modules. The results obtained by the proposed CGBO algorithm are compared with other state-of-the-art algorithms, such as GBO, MPA, EO, IMO, WOA, PSO, and IPSO. The simulation is carried out using MATLAB simulation software through Laptop with an i5 4th generation processor, 2.4 GHz clock frequency, and 8 GB memory. For all selected algorithms, the population is 40, and the maximum number of iterations is selected as 1000. For a fair comparison, each algorithm is run 30 times. For the GBO algorithm, the probability rate is selected as 0.5, as suggested

**TABLE 3.** Boundaries of different PV models.

Parameters	RTC Si Cell		PVM752 GaAs cell		Photowatt-PWP201		KC200GT & SM55	
	lb	ub	lb	ub	lb	ub	lb	ub
$I_p$ (A)	0	1	0	0.5	0	2	0	$2I_{sc}$
$I_{sd1}, I_{sd2}$ (A)	0	1e-06	0	1e-6	0	50e-06	0	100e-06
$a, a_1, a_2$	1	2	1	2	1	50	1	5
$R_p$ ( $\Omega$ )	0	100	0	1000	0	2000	0	5000
$R_s$ ( $\Omega$ )	0	0.5	0	0.8	0	2	0	2

$I_{sc}$ =Short-circuit current, lb-lower bound, ub-upper bound

**TABLE 4.** Decision variables of SDeM of the RTC France Si PV cell.

Algorithm	$I_p$ (A)	$I_{sd}$ (A)	$R_s$ ( $\Omega$ )	$R_p$ ( $\Omega$ )	$a$	RMSE
<b>CGBO</b>	0.760 8	3.23E-07	0.036	53.718	1.481	9.8602 E-04
<b>GBO</b>	0.760 8	3.23E-07	0.036	53.718	1.481	9.8602 E-04
<b>IMO</b>	0.760 2	5.22E-07	0.034	74.429	1.531	1.3932 E-03
<b>MPA</b>	0.760 7	9.49E-07	0.031	99.999	1.598	2.3408 E-03
<b>EO</b>	0.759 9	4.37E-07	0.035	81.219	1.512	1.2571 E-03
<b>WOA</b>	0.760 9	7.25E-07	0.032	97.010	1.567	2.4893 E-03
<b>PSO</b>	0.761 0	9.74E-07	0.031	103.47	1.601	2.3988 E-03
<b>IPSO</b>	0.760 8	0.0000 01	0.031 4	100.00 00	1.604 5	2.4480 E-03

by the inventor of the GBO algorithm. The control parameters of all other algorithms are selected based on literature and several trials. The parameter settings are listed in Table 2. The readers are encouraged to read the respective literature for more information about the control parameters.

A total of five different case studies are considered to validate the proposed CGBO algorithm. Case study 1 deals with SDeM and DDeM of the RTC France Si solar cell, case study 2 deals with SDeM and DDeM of the PVM752 GaAs cell, case study 3 deals with SDeM and DDeM of the Photowatt PWP-201 PV module, case study 4 deals with SDeM of the KC200GT PV module under different operating conditions, and case study 5 deals with SDeM of the SM55 PV module under various operating conditions. The lower and upper limits of different decision variables of PV cells and PV modules are listed in Table 3.

The performance of the algorithm is compared with other selected algorithms in terms of the RMSE, IAE, RE, runtime (RT), and convergence curve. A low value of RMSE indicates that the optimized data is nearer to the experimental data, i.e., the selected algorithm offers high efficiency in identifying the cell or module variables. Therefore, the error must be reduced as small as possible. RE and IAE are also used to highlight the error between the optimized data and the experimental sample at each voltage sample. The workflow

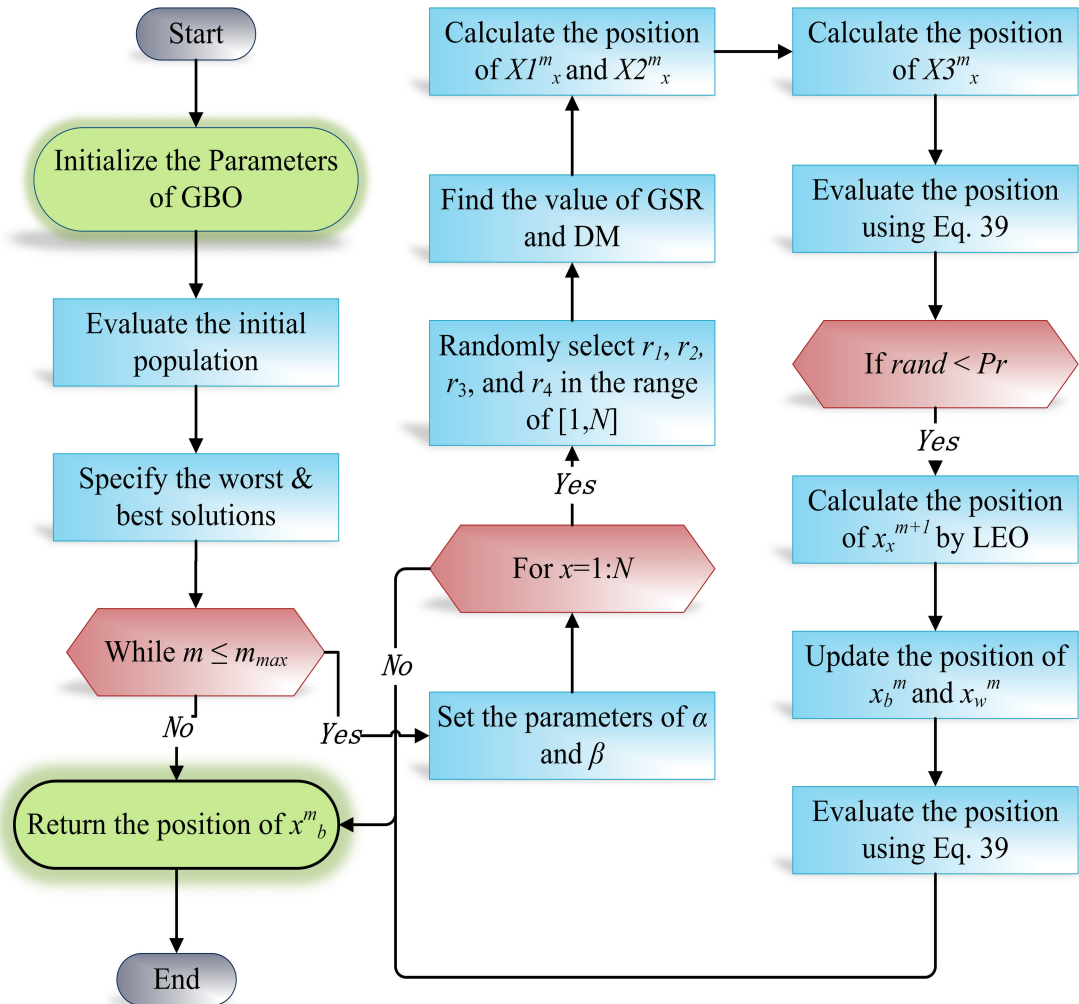


**FIGURE 5.** Flowchart of the proposed CGBO algorithm.

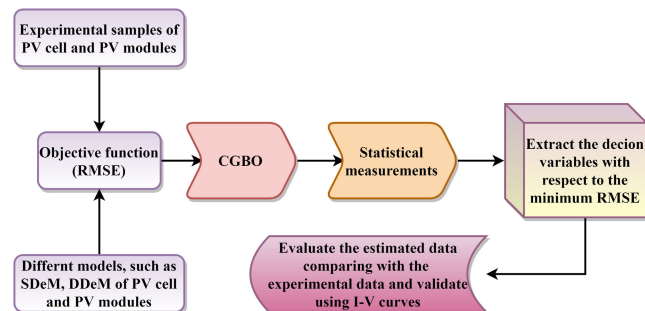


**FIGURE 6.** Workflow of PV parameters identification using CGBO algorithm.

of the CGBO application to identify the uncertain parameters of various PV models is illustrated in Fig. 6.

#### A. CASE STUDY-1

In this case study, the performance of the proposed CGBO algorithm is validated on SDeM and DDeM of the RTC France Si solar PV cell. For the simulation, 26 experimental samples are collected at 1000 W/m<sup>2</sup> irradiance and 33 °C

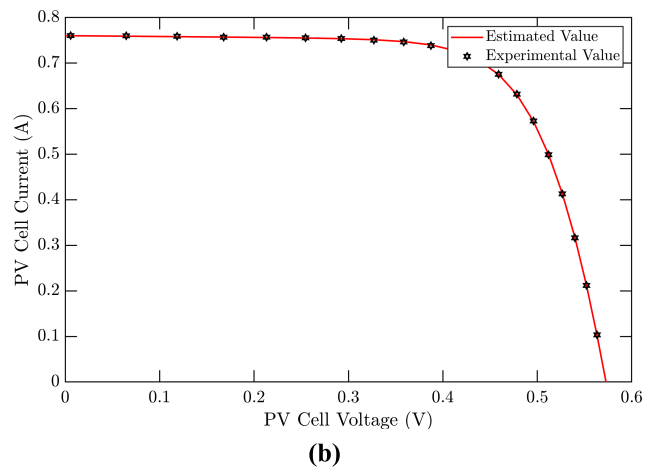
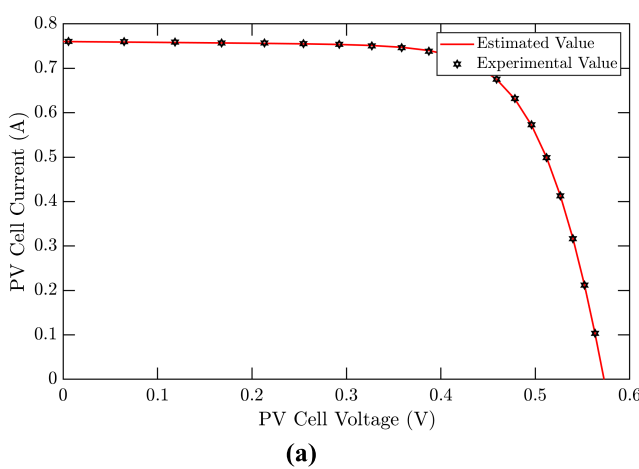
temperature. As discussed earlier, each selected algorithm is run 30 times to get fair results. Each algorithm tries to minimize the RMSE value by optimizing five decision variables for SDeM or seven decision variables for DDeM. The decision variables optimized by all selected algorithms are listed in Table 4 and Table 6. It is observed from Table 4 that both GBO and the proposed CGBO produce the same error for SDeM, i.e., 9.8602E-04; however, the proposed CGBO is better than GBO in terms of reliability and convergence speed. From Table 6, it is observed that the proposed CGBO algorithm produces less RMSE value, i.e., 9.8251E-04. In addition to RMSE, the proposed CGBO algorithm also gives very less RE, IAE<sub>i</sub>, and IAE<sub>p</sub>, as listed in Table 5 (for SDeM) and Table 7 (for DDeM). For SDeM of the RTC France Si PV cell, the average values of RE, IAE<sub>i</sub>, and IAE<sub>p</sub> are 4.74E-03, 8.28E-04, and 3.36 E-04, respectively, and for DDeM of the RTC France Si PV cell, the average values of RE, IAE<sub>i</sub>, and IAE<sub>p</sub> are 4.47E-03, 8.18E-04, and 8.78 E-04, respectively. In order to visualize the I-V characteristics of both SDeM and DDeM of the PV cell, the characteristic curves are illustrated in Fig. 7. From Fig. 7,

**TABLE 5.** RE and IAE of SDeM of the RTC france Si PV cell.

V <sub>act</sub> (V)	I <sub>act</sub> (A)	I <sub>est</sub> (A)	IAE <sub>i</sub>	RE	P <sub>act</sub> (W)	P <sub>est</sub> (W)	IAE <sub>p</sub>
-0.2057	0.7640	0.7641	8.77E-05	-1.15E-04	-0.1572	-0.1572	1.80E-05
-0.1291	0.7620	0.7627	6.63E-04	-8.70E-04	-0.0984	-0.0985	8.56E-05
-0.0588	0.7605	0.7614	8.55E-04	-1.12E-03	-0.0447	-0.0448	5.03E-05
0.0057	0.7605	0.7602	3.46E-04	4.55E-04	0.0043	0.0043	1.97E-06
0.0646	0.7600	0.7591	9.45E-04	1.24E-03	0.0491	0.0490	6.10E-05
0.1185	0.7590	0.7580	9.58E-04	1.26E-03	0.0899	0.0898	1.13E-04
0.1678	0.7570	0.7571	9.17E-05	-1.21E-04	0.1270	0.1270	1.54E-05
0.2132	0.7570	0.7561	8.59E-04	1.13E-03	0.1614	0.1612	1.83E-04
0.2545	0.7555	0.7551	4.13E-04	5.47E-04	0.1923	0.1922	1.05E-04
0.2924	0.7540	0.7537	3.36E-04	4.46E-04	0.2205	0.2204	9.83E-05
0.3269	0.7505	0.7514	8.91E-04	-1.19E-03	0.2453	0.2456	2.91E-04
0.3585	0.7465	0.7474	8.54E-04	-1.14E-03	0.2676	0.2679	3.06E-04
0.3873	0.7385	0.7401	1.62E-03	-2.19E-03	0.2860	0.2866	6.26E-04
0.4137	0.7280	0.7274	6.18E-04	8.49E-04	0.3012	0.3009	2.56E-04
0.4373	0.7065	0.7070	4.73E-04	-6.69E-04	0.3090	0.3092	2.07E-04
0.4590	0.6755	0.6753	2.20E-04	3.25E-04	0.3101	0.3100	1.01E-04
0.4784	0.6320	0.6308	1.24E-03	1.96E-03	0.3023	0.3018	5.94E-04
0.4960	0.5730	0.5719	1.07E-03	1.87E-03	0.2842	0.2837	5.32E-04
0.5119	0.4990	0.4996	6.07E-04	-1.22E-03	0.2554	0.2557	3.11E-04
0.5265	0.4130	0.4136	6.49E-04	-1.57E-03	0.2174	0.2178	3.42E-04
0.5398	0.3165	0.3175	1.01E-03	-3.19E-03	0.1708	0.1714	5.45E-04
0.5521	0.2120	0.2122	1.55E-04	-7.31E-04	0.1170	0.1171	8.55E-05
0.5633	0.1035	0.1023	1.25E-03	1.21E-02	0.0583	0.0576	7.03E-04
0.5736	-0.0100	-0.0087	1.28E-03	1.28E-01	-0.0057	-0.0050	7.36E-04
0.5833	-0.1230	-0.1255	2.51E-03	-2.04E-02	-0.0717	-0.0732	1.46E-03
0.5900	-0.2100	-0.2085	1.53E-03	7.27E-03	-0.1239	-0.1230	9.01E-04
Sum of error		8.28E-04	4.74E-03	-	-	-	3.36E-04

**TABLE 6.** Decision variables of DDeM of the RTC france Si PV cell.

Algorithm	I <sub>p</sub> (A)	I <sub>sdl</sub> (A)	R <sub>s</sub> ( $\Omega$ )	R <sub>p</sub> ( $\Omega$ )	a <sub>1</sub>	I <sub>s2</sub> (A)	a <sub>2</sub>	RMSE
<b>CGBO</b>	0.7608	2.2E-07	0.0368	55.5658	1.4488	8.012E-07	2	9.8251E-04
<b>GBO</b>	0.7608	5.28E-08	0.0364	53.9455	1.7980	3.071E-07	1.4773	9.8566E-04
<b>IMO</b>	0.7602	7.81E-07	0.0323	86.8312	1.5759	0	1.5892	2.0593E-03
<b>MPA</b>	0.7602	4.52E-08	0.0387	60.6960	1.3342	6.667E-07	1.7063	1.2771E-03
<b>EO</b>	0.7604	4.63E-07	0.0349	71.7118	1.5182	1.442E-09	1.9827	1.2200E-03
<b>WOA</b>	0.7881	7.4E-08	0.0337	7.6252	1.4298	5.84E-07	1.6110	2.0085E-02
<b>PSO</b>	0.7630	8.42E-07	0.0309	70.6572	1.5917	8.944E-07	2	3.0555E-03
<b>IPSO</b>	0.7615	0.000001	0.0300	100.0000	2.0000	0.000001	1.6130	3.1263E-03

**FIGURE 7.** I-V characteristic curves of the RTC France Si cell; (a) SDeM, (b) DDeM.

it is observed that the experimental sample and estimated data are matching accurately. Therefore, from the above-all discussions, it is proved that the proposed CGBO algorithm

is superior to all selected algorithms. Next to the CGBO algorithm, the performance of GBO is better than all other algorithms.

**TABLE 7.** RE and IAE of DDeM of the RTC france Si PV cell.

V <sub>act</sub> (V)	I <sub>act</sub> (A)	I <sub>est</sub> (A)	IAE <sub>i</sub>	RE	P <sub>act</sub> (W)	P <sub>est</sub> (W)	IAE <sub>p</sub>
-0.2057	0.7640	0.7640	1.59E-05	2.08E-05	-0.1572	-0.1572	3.27E-06
-0.1291	0.7620	0.7626	6.07E-04	-7.96E-04	-0.0984	-0.0985	7.83E-05
-0.0588	0.7605	0.7613	8.42E-04	-1.11E-03	-0.0447	-0.0448	4.95E-05
0.0057	0.7605	0.7602	3.20E-04	4.21E-04	0.0043	0.0043	1.82E-06
0.0646	0.7600	0.7591	8.85E-04	1.16E-03	0.0491	0.0490	5.72E-05
0.1185	0.7590	0.7581	8.70E-04	1.15E-03	0.0899	0.0898	1.03E-04
0.1678	0.7570	0.7572	1.98E-04	-2.61E-04	0.1270	0.1271	3.32E-05
0.2132	0.7570	0.7563	7.48E-04	9.88E-04	0.1614	0.1612	1.59E-04
0.2545	0.7555	0.7552	3.16E-04	4.18E-04	0.1923	0.1922	8.03E-05
0.2924	0.7540	0.7537	2.74E-04	3.63E-04	0.2205	0.2204	8.00E-05
0.3269	0.7505	0.7514	8.99E-04	-1.20E-03	0.2453	0.2456	2.94E-04
0.3585	0.7465	0.7473	7.97E-04	-1.07E-03	0.2676	0.2679	2.86E-04
0.3873	0.7385	0.7400	1.50E-03	-2.03E-03	0.2860	0.2866	5.82E-04
0.4137	0.7280	0.7272	7.64E-04	1.05E-03	0.3012	0.3009	3.16E-04
0.4373	0.7065	0.7068	3.40E-04	-4.82E-04	0.3090	0.3091	1.49E-04
0.4590	0.6755	0.6752	2.95E-04	4.37E-04	0.3101	0.3099	1.35E-04
0.4784	0.6320	0.6308	1.24E-03	1.96E-03	0.3023	0.3018	5.93E-04
0.4960	0.5730	0.5720	1.00E-03	1.74E-03	0.2842	0.2837	4.96E-04
0.5119	0.4990	0.4997	7.14E-04	-1.43E-03	0.2554	0.2558	3.66E-04
0.5265	0.4130	0.4137	7.41E-04	-1.79E-03	0.2174	0.2178	3.90E-04
0.5398	0.3165	0.3175	1.05E-03	-3.32E-03	0.1708	0.1714	5.67E-04
0.5521	0.2120	0.2121	1.21E-04	-5.72E-04	0.1170	0.1171	6.69E-05
0.5633	0.1035	0.1022	1.34E-03	1.30E-02	0.0583	0.0575	7.56E-04
0.5736	-0.0100	-0.0088	1.20E-03	1.20E-01	-0.0057	-0.0050	6.90E-04
0.5833	-0.1230	-0.1255	2.54E-03	-2.07E-02	-0.0717	-0.0732	1.48E-03
0.5900	-0.2100	-0.2084	1.64E-03	7.80E-03	-0.1239	-0.1229	9.67E-04
<b>Sum of error</b>		<b>8.18E-04</b>	<b>4.47E-03</b>	-	-	<b>8.78E-03</b>	

**TABLE 8.** Decision variables of SDeM of the PVM752 GaAs solar cell.

Algorithm	I <sub>p</sub> (A)	I <sub>sd</sub> (A)	R <sub>s</sub> ( $\Omega$ )	R <sub>p</sub> ( $\Omega$ )	a	RMSE
<b>CGBO</b>	0.0999	7.12E-12	0.6477	907.3413	1.6592	2.52E-04
<b>GBO</b>	0.0999	7.85E-12	0.6454	882.1252	1.6662	2.53E-04
<b>IMO</b>	0.1140	0.00E+00	0.0000	14.5082	1.0122	2.54E-02
<b>MPA</b>	0.1000	1.15E-11	0.6343	815.3168	1.6939	2.67E-04
<b>EO</b>	0.1138	0.00E+00	0.0000	14.5886	1.9967	2.54E-02
<b>WOA</b>	0.1017	2.32E-10	0.5176	196.9917	1.9525	1.30E-03
<b>PSO</b>	0.0085	-1.16E-03	-165.1620	184.5858	-423.9039	1.92E-03
<b>IPSO</b>	0.1138	0.00E+00	0.0000	14.5886	2.0000	2.54E-02

**B. CASE STUDY-2**

In this case study, the performance of the proposed CGBO algorithm is validated on SDeM and DDeM of the PVM752 GaAs solar cell. For the simulation, 44 experimental samples are collected at 1000 W/m<sup>2</sup> irradiance and 25 °C temperature. Each algorithm tries to minimize the RMSE value by optimizing five decision variables for SDeM or seven decision variables for DDeM. The decision variables

optimized by all selected algorithms are listed in Table 8 and Table 10. It is observed from Table 8 that the proposed CGBO algorithm can obtain minimum RMSE for SDeM, i.e., 2.52E-04, and from Table 10, it is observed that the proposed CGBO algorithm can obtain less RMSE value, i.e., 2.22E-04. It is also observed from Table 8 and Table 10 that the PSO algorithms search the optimal solution outside the search space, which is not suitable for parameter estimation

**TABLE 9.** RE and IAE of SDeM of the PVM752 GaAs solar cell.

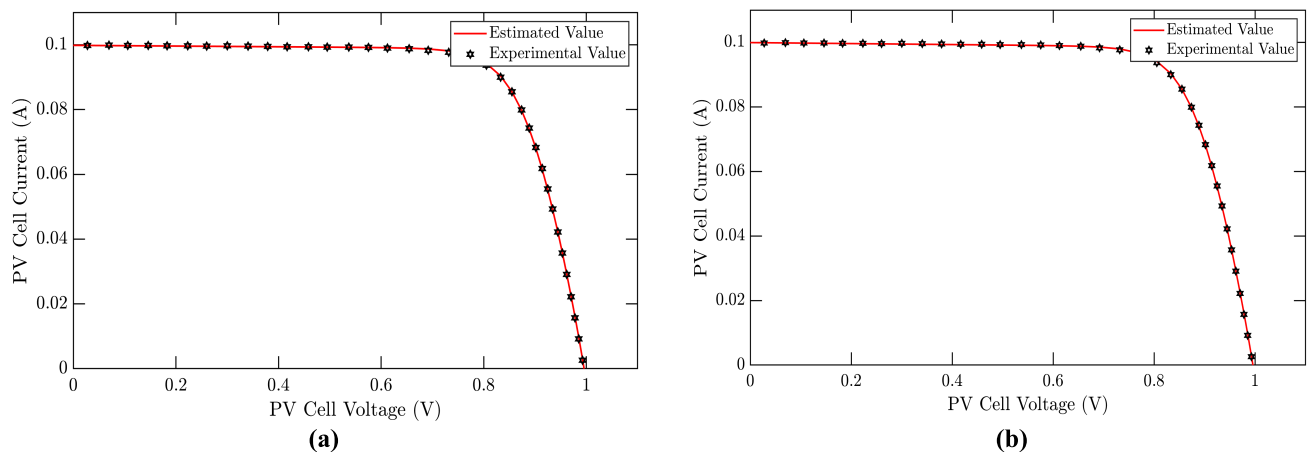
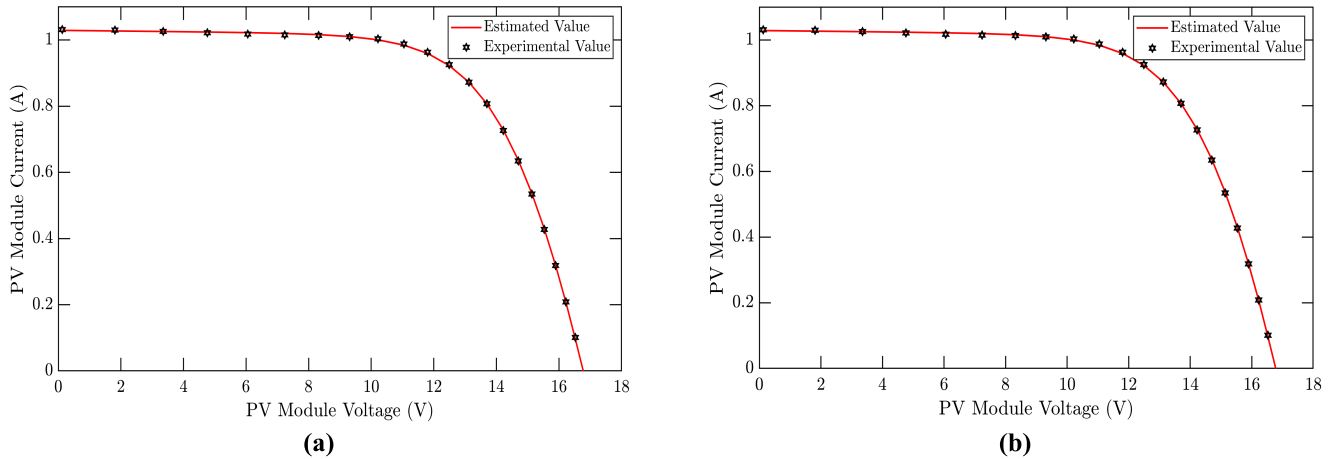
V <sub>act</sub> (V)	I <sub>act</sub> (A)	I <sub>est</sub> (A)	IAE <sub>i</sub>	RE	P <sub>act</sub> (W)	P <sub>est</sub> (W)	IAE <sub>p</sub>
-0.1659	0.1001	0.1000	8.06E-05	8.05E-04	-0.0166	-0.0166	1.34E-05
-0.1281	0.1000	0.1000	2.22E-05	2.22E-04	-0.0128	-0.0128	2.85E-06
-0.0888	0.0999	0.0999	3.45E-05	-3.46E-04	-0.0089	-0.0089	3.07E-06
-0.0490	0.0999	0.0999	9.32E-06	9.33E-05	-0.0049	-0.0049	4.57E-07
-0.0102	0.0999	0.0998	5.21E-05	5.21E-04	-0.0010	-0.0010	5.31E-07
0.0275	0.0998	0.0998	6.44E-06	-6.45E-05	0.0027	0.0027	1.77E-07
0.0695	0.0999	0.0998	1.40E-04	1.40E-03	0.0069	0.0069	9.72E-06
0.1061	0.0998	0.0997	8.02E-05	8.03E-04	0.0106	0.0106	8.51E-06
0.1460	0.0998	0.0997	1.24E-04	1.24E-03	0.0146	0.0146	1.81E-05
0.1828	0.0997	0.0996	6.47E-05	6.48E-04	0.0182	0.0182	1.18E-05
0.2230	0.0997	0.0996	1.09E-04	1.09E-03	0.0222	0.0222	2.43E-05
0.2600	0.0996	0.0996	4.97E-05	4.99E-04	0.0259	0.0259	1.29E-05
0.3001	0.0997	0.0995	1.94E-04	1.95E-03	0.0299	0.0299	5.82E-05
0.3406	0.0996	0.0995	1.39E-04	1.39E-03	0.0339	0.0339	4.72E-05
0.3789	0.0995	0.0994	8.09E-05	8.13E-04	0.0377	0.0377	3.06E-05
0.4168	0.0994	0.0994	2.29E-05	2.30E-04	0.0414	0.0414	9.54E-06
0.4583	0.0994	0.0993	6.96E-05	7.00E-04	0.0456	0.0455	3.19E-05
0.4949	0.0993	0.0993	1.19E-05	1.20E-04	0.0491	0.0491	5.88E-06
0.5370	0.0993	0.0992	6.42E-05	6.47E-04	0.0533	0.0533	3.45E-05
0.5753	0.0992	0.0992	2.02E-05	2.04E-04	0.0571	0.0571	1.16E-05
0.6123	0.0990	0.0991	1.07E-04	-1.08E-03	0.0606	0.0607	6.56E-05
0.6546	0.0988	0.0990	1.67E-04	-1.69E-03	0.0647	0.0648	1.09E-04
0.6918	0.0983	0.0987	4.22E-04	-4.29E-03	0.0680	0.0683	2.92E-04
0.7318	0.0977	0.0981	4.36E-04	-4.46E-03	0.0715	0.0718	3.19E-04
0.7702	0.0963	0.0968	5.31E-04	-5.51E-03	0.0742	0.0746	4.09E-04
0.8053	0.0937	0.0942	5.25E-04	-5.60E-03	0.0755	0.0759	4.23E-04
0.8329	0.0900	0.0904	3.85E-04	-4.27E-03	0.0750	0.0753	3.20E-04
0.8550	0.0855	0.0855	8.87E-06	-1.04E-04	0.0731	0.0731	7.59E-06
0.8738	0.0799	0.0798	1.35E-04	1.68E-03	0.0698	0.0697	1.18E-04
0.8887	0.0743	0.0740	3.35E-04	4.51E-03	0.0660	0.0657	2.98E-04
0.9016	0.0683	0.0681	2.11E-04	3.08E-03	0.0616	0.0614	1.90E-04
0.9141	0.0618	0.0615	3.26E-04	5.28E-03	0.0565	0.0562	2.98E-04
0.9248	0.0555	0.0552	3.13E-04	5.64E-03	0.0513	0.0510	2.89E-04
0.9344	0.0493	0.0491	2.30E-04	4.67E-03	0.0461	0.0459	2.15E-04
0.9445	0.0422	0.0422	7.90E-06	-1.87E-04	0.0399	0.0399	7.46E-06
0.9533	0.0357	0.0358	6.54E-05	-1.83E-03	0.0340	0.0341	6.23E-05
0.9618	0.0291	0.0292	8.99E-05	-3.09E-03	0.0280	0.0281	8.65E-05
0.9702	0.0222	0.0225	2.59E-04	-1.17E-02	0.0215	0.0218	2.51E-04
0.9778	0.0157	0.0161	4.35E-04	-2.77E-02	0.0154	0.0158	4.25E-04
0.9852	0.0092	0.0097	5.07E-04	-5.51E-02	0.0091	0.0096	5.00E-04
0.9926	0.0026	0.0029	3.26E-04	-1.25E-01	0.0026	0.0029	3.24E-04
0.9999	-0.0040	-0.0041	1.29E-04	-3.21E-02	-0.0040	-0.0041	1.29E-04
1.0046	-0.0085	-0.0085	3.30E-05	-3.88E-03	-0.0085	-0.0086	3.31E-05
1.0089	-0.0124	-0.0131	6.96E-04	-5.61E-02	-0.0125	-0.0132	7.02E-04
<b>Sum of error</b>		<b>1.83E-04</b>	<b>-6.96E-03</b>	-	-	<b>1.41E-04</b>	

problems. Therefore, the PSO algorithm requires an effective constraint handling mechanism to bring the particles inside the search space. In addition, the improved PSO algorithm fails to optimize the parameter estimation problem. It is wholly stuck at local optima, and it could not find the optimal global solution. As similar to PSO, an improved PSO is also not suitable for parameter estimation problems. In addition to RMSE, the proposed CGBO algorithm also gives very less

RE, IAE<sub>i</sub>, and IAE<sub>p</sub>, as listed in Table 9 (for SDeM) and Table 11 (for DDeM). For SDeM of the PVM752 GaAs solar cell, the average values of RE, IAE<sub>i</sub>, and IAE<sub>p</sub> are 6.96E-03, 1.83E-04, and 1.41E-04, respectively, and for DDeM of the PVM752 GaAs solar cell, the average values of RE, IAE<sub>i</sub>, and IAE<sub>p</sub> are 6.94E-03, 1.82E-04, and 5.81E-03, respectively. In order to visualize the I-V characteristics of both SDeM and DDeM of the PVM752 GaAs solar cell, the characteristic

**TABLE 10.** Decision variables of DDeM of the PVM752 GaAs solar cell.

Algorithm	$I_p$ (A)	$I_{sd1}$ (A)	$R_s$ ( $\Omega$ )	$R_p$ ( $\Omega$ )	$a_1$	$I_{sd2}$ (A)	$a_2$	RMSE
<b>CGBO</b>	0.1000	5.27E-12	0.6520	656.0251	1.6383	0.00E+00	1.0000	2.22E-04
<b>GBO</b>	0.0999	7.19E-14	0.6724	997.9138	1.4087	1.36E-10	2.0000	2.32E-04
<b>IMO</b>	0.1041	0.00E+00	0.0000	52.5857	2.0000	3.36E-10	2.0000	6.68E-03
<b>MPA</b>	0.1001	7.04E-14	0.5260	981.9015	1.9995	3.47E-10	1.9902	6.86E-04
<b>EO</b>	0.1138	0.00E+00	0.0000	14.5886	1.1436	0.00E+00	1.9693	2.54E-02
<b>WOA</b>	0.1006	0.00E+00	0.6884	894.2582	1.9146	1.83E-10	1.9297	2.91E-03
<b>PSO</b>	0.0606	-2.45E-02	-16.5257	503.0909	18.9910	6.90E-02	26.6620	3.30E-03
<b>IPSO</b>	0.5000	1.00E-06	0.0000	1000	2	1.00E-06	2	215.11

**FIGURE 8.** I-V characteristic curves of the PVM752 GaAs solar cell; (a) SDeM, (b) DdeM.**FIGURE 9.** I-V characteristic curves of the Photowatt-PWP-201 PV module; (a) SDeM, (b) DdeM.

curves are illustrated in Fig. 8. From Fig. 8, it is observed that the experimental sample and estimated data are matching accurately. Therefore, from the above-all discussions, it is proved that the proposed CGBO algorithm is superior

to all selected algorithms for the estimation of uncertain variables of PVM752 GaAs solar cell. Next to the CGBO algorithm, the performance of GBO is better than all other algorithms.

**TABLE 11.** RE and IAE of DDeM of the PVM752 GaAs solar cell.

V <sub>act</sub> (V)	I <sub>act</sub> (A)	I <sub>est</sub> (A)	IAE <sub>i</sub>	RE	P <sub>act</sub> (W)	P <sub>est</sub> (W)	IAE <sub>p</sub>
-0.1659	0.1001	0.1002	8.19E-05	-8.18E-04	-0.0166	-0.0166	1.36E-05
-0.1281	0.1000	0.1001	1.24E-04	-1.24E-03	-0.0128	-0.0128	1.59E-05
-0.0888	0.0999	0.1001	1.65E-04	-1.65E-03	-0.0089	-0.0089	1.46E-05
-0.0490	0.0999	0.1000	1.04E-04	-1.04E-03	-0.0049	-0.0049	5.09E-06
-0.0102	0.0999	0.0999	4.47E-05	-4.48E-04	-0.0010	-0.0010	4.56E-07
0.0275	0.0998	0.0999	8.74E-05	-8.76E-04	0.0027	0.0027	2.40E-06
0.0695	0.0999	0.0998	7.67E-05	7.68E-04	0.0069	0.0069	5.33E-06
0.1061	0.0998	0.0998	3.24E-05	3.25E-04	0.0106	0.0106	3.44E-06
0.1460	0.0998	0.0997	9.33E-05	9.34E-04	0.0146	0.0146	1.36E-05
0.1828	0.0997	0.0997	4.93E-05	4.94E-04	0.0182	0.0182	9.00E-06
0.2230	0.0997	0.0996	1.11E-04	1.11E-03	0.0222	0.0222	2.46E-05
0.2600	0.0996	0.0995	6.68E-05	6.71E-04	0.0259	0.0259	1.74E-05
0.3001	0.0997	0.0995	2.28E-04	2.29E-03	0.0299	0.0299	6.84E-05
0.3406	0.0996	0.0994	1.90E-04	1.91E-03	0.0339	0.0339	6.46E-05
0.3789	0.0995	0.0994	1.48E-04	1.49E-03	0.0377	0.0376	5.61E-05
0.4168	0.0994	0.0993	1.06E-04	1.07E-03	0.0414	0.0414	4.42E-05
0.4583	0.0994	0.0992	1.70E-04	1.71E-03	0.0456	0.0455	7.80E-05
0.4949	0.0993	0.0992	1.28E-04	1.29E-03	0.0491	0.0491	6.32E-05
0.5370	0.0993	0.0991	1.97E-04	1.99E-03	0.0533	0.0532	1.06E-04
0.5753	0.0992	0.0990	1.68E-04	1.70E-03	0.0571	0.0570	9.67E-05
0.6123	0.0990	0.0989	5.40E-05	5.45E-04	0.0606	0.0606	3.30E-05
0.6546	0.0988	0.0988	5.63E-06	5.70E-05	0.0647	0.0647	3.69E-06
0.6918	0.0983	0.0985	2.45E-04	-2.49E-03	0.0680	0.0682	1.69E-04
0.7318	0.0977	0.0980	2.66E-04	-2.72E-03	0.0715	0.0717	1.95E-04
0.7702	0.0963	0.0967	3.88E-04	-4.03E-03	0.0742	0.0745	2.99E-04
0.8053	0.0937	0.0941	4.29E-04	-4.58E-03	0.0755	0.0758	3.45E-04
0.8329	0.0900	0.0903	3.39E-04	-3.77E-03	0.0750	0.0752	2.83E-04
0.8550	0.0855	0.0855	6.06E-06	-7.09E-05	0.0731	0.0731	5.19E-06
0.8738	0.0799	0.0798	1.07E-04	1.33E-03	0.0698	0.0697	9.32E-05
0.8887	0.0743	0.0740	2.91E-04	3.91E-03	0.0660	0.0658	2.58E-04
0.9016	0.0683	0.0681	1.58E-04	2.32E-03	0.0616	0.0614	1.43E-04
0.9141	0.0618	0.0615	2.74E-04	4.43E-03	0.0565	0.0562	2.50E-04
0.9248	0.0555	0.0552	2.65E-04	4.78E-03	0.0513	0.0511	2.45E-04
0.9344	0.0493	0.0491	1.90E-04	3.85E-03	0.0461	0.0459	1.77E-04
0.9445	0.0422	0.0422	3.87E-05	-9.16E-04	0.0399	0.0399	3.65E-05
0.9533	0.0357	0.0358	8.56E-05	-2.40E-03	0.0340	0.0341	8.16E-05
0.9618	0.0291	0.0292	9.94E-05	-3.41E-03	0.0280	0.0281	9.56E-05
0.9702	0.0222	0.0225	2.60E-04	-1.17E-02	0.0215	0.0218	2.52E-04
0.9778	0.0157	0.0161	4.29E-04	-2.73E-02	0.0154	0.0158	4.20E-04
0.9852	0.0092	0.0097	4.96E-04	-5.39E-02	0.0091	0.0096	4.89E-04
0.9926	0.0026	0.0029	3.10E-04	-1.19E-01	0.0026	0.0029	3.07E-04
0.9999	-0.0040	-0.0042	1.50E-04	-3.75E-02	-0.0040	-0.0041	1.50E-04
1.0046	-0.0085	-0.0086	5.20E-05	-6.11E-03	-0.0085	-0.0086	5.22E-05
1.0089	-0.0124	-0.0131	7.19E-04	-5.80E-02	-0.0125	-0.0132	7.25E-04
<b>Sum of error</b>		<b>1.82E-04</b>	<b>-6.94E-03</b>	-	-	<b>5.81E-03</b>	

**C. CASE STUDY-3**

In this case study, the performance of the proposed CGBO algorithm is validated on SDeM and DDeM of

the Photowatt-PWP-201 PV module. For the simulation, 25 experimental samples are collected at 1000 W/m<sup>2</sup> irradiance and 45 °C temperature. The decision variables optimized

**TABLE 12.** Decision variables of SDeM of the Photowatt-PWP-201 PV module.

Algorithm	$I_p$ (A)	$I_{sd}$ (A)	$R_s$ ( $\Omega$ )	$R_p$ ( $\Omega$ )	$a$	RMSE
<b>CGBO</b>	1.0305	3.48E-06	1.2013	981.9821	48.6428	2.4251E-03
<b>GBO</b>	1.0305	3.48E-06	1.2013	981.9821	48.6428	2.4251E-03
<b>IMO</b>	1.0264	3.45E-06	1.2112	1899.6737	48.5924	2.7593E-03
<b>MPA</b>	1.0273	4.51E-06	1.1781	1977.6535	49.6486	2.5934E-03
<b>EO</b>	1.0296	3.76E-06	1.1943	1139.0284	48.9340	2.4385E-03
<b>WOA</b>	1.0280	4.75E-06	1.1680	1712.8543	49.8593	2.5914E-03
<b>PSO</b>	1.0263	2.76E-06	1.2392	1655.6278	47.7452	3.0801E-03
<b>IPSO</b>	1.0286	4.92E-06	1.1646	1589.2728	50.0000	2.6081E-03

**TABLE 13.** RE and IAE of SDeM of the Photowatt-PWP-201 PV module.

$V_{act}$ (V)	$I_{act}$ (A)	$I_{est}$ (A)	IAE <sub>i</sub>	RE	$P_{act}$ (W)	$P_{est}$ (W)	IAE <sub>p</sub>
0.1248	1.0315	1.0291	2.38E-03	2.31E-03	0.1287	0.1284	2.97E-04
1.8093	1.0300	1.0274	2.62E-03	2.54E-03	1.8636	1.8588	4.74E-03
3.3511	1.0260	1.0257	2.58E-04	2.52E-04	3.4382	3.4374	8.65E-04
4.7622	1.0220	1.0241	2.11E-03	-2.06E-03	4.8670	4.8770	1.00E-02
6.0538	1.0180	1.0223	4.29E-03	4.22E-03	6.1628	6.1888	2.60E-02
7.2364	1.0155	1.0199	4.43E-03	-4.36E-03	7.3486	7.3806	3.21E-02
8.3189	1.0140	1.0164	2.36E-03	-2.33E-03	8.4354	8.4550	1.97E-02
9.3097	1.0100	1.0105	4.96E-04	-4.91E-04	9.4028	9.4074	4.62E-03
10.2163	1.0035	1.0006	2.87E-03	2.86E-03	10.2521	10.2227	2.93E-02
11.0449	0.9880	0.9845	3.45E-03	3.49E-03	10.9124	10.8742	3.81E-02
11.8018	0.9630	0.9595	3.48E-03	3.61E-03	11.3651	11.3241	4.11E-02
12.4929	0.9255	0.9228	2.66E-03	2.88E-03	11.5622	11.5289	3.32E-02
13.1231	0.8725	0.8726	9.97E-05	-1.14E-04	11.4499	11.4512	1.31E-03
13.6983	0.8075	0.8073	2.26E-04	2.80E-04	11.0614	11.0583	3.09E-03
14.2221	0.7265	0.7283	1.84E-03	-2.53E-03	10.3324	10.3585	2.61E-02
14.6995	0.6345	0.6371	2.64E-03	-4.16E-03	9.3268	9.3656	3.88E-02
15.1346	0.5345	0.5362	1.71E-03	-3.20E-03	8.0894	8.1154	2.59E-02
15.5311	0.4275	0.4295	2.01E-03	-4.70E-03	6.6395	6.6708	3.12E-02
15.8929	0.3185	0.3188	2.74E-04	-8.62E-04	5.0619	5.0663	4.36E-03
16.2229	0.2085	0.2074	1.11E-03	5.33E-03	3.3825	3.3645	1.80E-02
16.5241	0.1010	0.0962	4.83E-03	4.78E-02	1.6689	1.5891	7.99E-02
16.7987	-0.0080	-0.0083	3.25E-04	-4.07E-02	-0.1344	-0.1399	5.47E-03
17.0499	-0.1110	-0.1109	6.35E-05	5.72E-04	-1.8925	-1.8915	1.08E-03
17.2793	-0.2090	-0.2092	2.47E-04	-1.18E-03	-3.6114	-3.6156	4.27E-03
17.4885	-0.3030	-0.3009	2.14E-03	7.05E-03	-5.2990	-5.2617	3.74E-02
<b>Sum of error</b>		<b>1.96E-03</b>	<b>3.25E-04</b>	-	-	<b>2.07E-02</b>	

**TABLE 14.** Decision variables of DDeM of the Photowatt-PWP-201 PV module.

Algorithm	$I_p$ (A)	$I_{sd1}$ (A)	$R_s$ ( $\Omega$ )	$R_p$ ( $\Omega$ )	$a_1$	$I_{sd2}$ (A)	$a_2$	RMSE
<b>CGBO</b>	1.0305	3.48E-06	1.2013	981.8874	48.6428	3.89E-12	34.7828	2.4251E-03
<b>GBO</b>	1.0305	3.47E-06	1.2016	981.2677	48.6314	0.00E+00	50.0000	2.4251E-03
<b>IMO</b>	1.0251	0.00E+00	1.2339	1849.8346	45.7618	3.07E-06	48.1472	3.3063E-03
<b>MPA</b>	1.0276	9.71E-13	1.1676	1965.5137	48.1139	4.89E-06	49.9760	2.6227E-03
<b>EO</b>	1.0288	9.38E-10	1.1896	1310.6705	47.1325	3.96E-06	49.1369	2.4687E-03
<b>WOA</b>	0.9903	0.00E+00	0.0000	202.8633	1.0256	4.04E-06	50.0000	8.9973E-02
<b>PSO</b>	1.0314	3.14E-06	1.1944	694.6947	48.6684	2.61E-07	47.6085	3.2066E-03
<b>IPSO</b>	1.0286	4.92E-06	1.1646	1589.2728	50.0000	0.00E+00	50.0000	2.6081E-03

by all selected algorithms are listed in Table 12 and Table 14. It is observed from Table 12 that both GBO and the proposed CGBO produce the same error for SDeM, i.e., 2.4251E-04, and from Table 14, it is observed that both GBO and the

proposed CGBO produce the same error for DDeM, i.e., 2.4251E-04, however, the proposed CGBO is better than GBO in terms of reliability and convergence speed. In addition to RMSE, the proposed CGBO algorithm also gives very

**TABLE 15.** RE and IAE of SDeM of the Photowatt-PWP-201 PV module.

V <sub>act</sub> (V)	I <sub>act</sub> (A)	I <sub>est</sub> (A)	IAE <sub>i</sub>	RE	P <sub>act</sub> (W)	P <sub>est</sub> (W)	IAE <sub>p</sub>
0.1248	1.0315	1.0291	2.38E-03	2.31E-03	0.1287	0.1284	2.97E-04
1.8093	1.0300	1.0274	2.62E-03	2.54E-03	1.8636	1.8588	4.74E-03
3.3511	1.0260	1.0257	2.58E-04	2.51E-04	3.4382	3.4374	8.64E-04
4.7622	1.0220	1.0241	2.11E-03	-2.06E-03	4.8670	4.8770	1.00E-02
6.0538	1.0180	1.0223	4.29E-03	-4.22E-03	6.1628	6.1888	2.60E-02
7.2364	1.0155	1.0199	4.43E-03	-4.36E-03	7.3486	7.3806	3.21E-02
8.3189	1.0140	1.0164	2.36E-03	-2.33E-03	8.4354	8.4550	1.97E-02
9.3097	1.0100	1.0105	4.96E-04	-4.91E-04	9.4028	9.4074	4.62E-03
10.2163	1.0035	1.0006	2.87E-03	2.86E-03	10.2521	10.2227	2.93E-02
11.0449	0.9880	0.9845	3.45E-03	3.49E-03	10.9124	10.8742	3.81E-02
11.8018	0.9630	0.9595	3.48E-03	3.61E-03	11.3651	11.3241	4.11E-02
12.4929	0.9255	0.9228	2.66E-03	2.88E-03	11.5622	11.5289	3.32E-02
13.1231	0.8725	0.8726	9.94E-05	-1.14E-04	11.4499	11.4512	1.30E-03
13.6983	0.8075	0.8073	2.26E-04	2.80E-04	11.0614	11.0583	3.10E-03
14.2221	0.7265	0.7283	1.84E-03	-2.53E-03	10.3324	10.3585	2.61E-02
14.6995	0.6345	0.6371	2.64E-03	-4.16E-03	9.3268	9.3656	3.88E-02
15.1346	0.5345	0.5362	1.71E-03	-3.21E-03	8.0894	8.1154	2.59E-02
15.5311	0.4275	0.4295	2.01E-03	-4.71E-03	6.6395	6.6708	3.12E-02
15.8929	0.3185	0.3188	2.75E-04	-8.62E-04	5.0619	5.0663	4.37E-03
16.2229	0.2085	0.2074	1.11E-03	5.33E-03	3.3825	3.3645	1.80E-02
16.5241	0.1010	0.0962	4.83E-03	4.78E-02	1.6689	1.5891	7.99E-02
16.7987	-0.0080	-0.0083	3.25E-04	-4.07E-02	-0.1344	-0.1399	5.46E-03
17.0499	-0.1110	-0.1109	6.35E-05	5.72E-04	-1.8925	-1.8915	1.08E-03
17.2793	-0.2090	-0.2092	2.47E-04	-1.18E-03	-3.6114	-3.6156	4.27E-03
17.4885	-0.3030	-0.3009	2.14E-03	7.05E-03	-5.2990	-5.2617	3.74E-02
<b>Sum of error</b>		<b>1.96E-03</b>	<b>3.26E-04</b>	-	-	<b>2.07E-02</b>	

**TABLE 16.** Decision variables of the KC200GT PV module obtained by all algorithms under different temperature conditions.

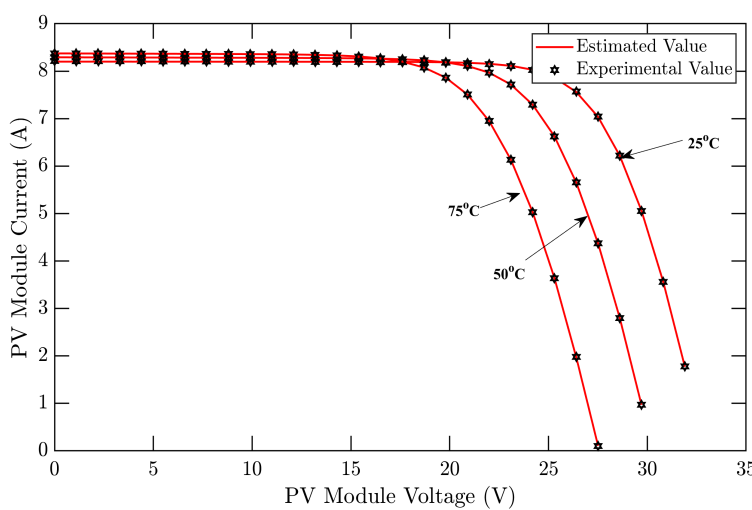
Condition	Algorithm	I <sub>p</sub> (A)	I <sub>sd</sub> (A)	R <sub>s</sub> ( $\Omega$ )	R <sub>p</sub> ( $\Omega$ )	a	RMSE
25°C	CGBO	8.201663	4.44E-09	0.333303	4986.789	1.110447	6.4518E-03
	GBO	8.204166	4.76E-09	0.332611	3345.386	1.1114105	6.7008E-03
	IMO	8.242908	1.23E-05	0.099476	4924.261	1.75354	8.5144E-02
	MPA	8.249296	2.94E-05	0.051183	4999.996	1.871542	9.6064E-02
	EO	8.223271	6.82E-07	0.208296	4894.759	1.447208	5.1490E-02
	WOA	8.251749	1.13E-05	0.100188	1063.135	1.741846	8.6519E-02
	PSO	8.292866	0.0001	0	2921.46	2.071981	1.1843E-01
	IPSO	8.270254	0.0001	0	5000	2.072842	1.1627E-01
	CGBO	8.295485	1.27E-07	0.335407	939.6941	1.118015	2.7581E-03
	GBO	8.296133	1.33E-07	0.334352	921.2209	1.120685	2.8869E-03
50°C	IMO	8.327198	2.12E-05	0.174989	1104.461	1.555261	7.5538E-02
	MPA	8.318867	1.28E-05	0.205016	4999.977	1.498695	6.3988E-02
	EO	8.301606	1.25E-06	0.284106	4955.469	1.278928	2.8887E-02
	WOA	8.330168	1.6E-05	0.211722	1284.815	1.525678	7.4918E-02
	PSO	8.319941	0.0001	0	3474.577	1.752048	1.7907E-01
	IPSO	8.340337	0.0001	0.108664	5000	1.765758	9.9118E-02
	CGBO	8.378164	1.62E-06	0.342598	767.1287	1.101049	4.4558E-03
	GBO	8.377664	1.63E-06	0.342497	790.4933	1.101481	4.4729E-03
	IMO	8.397435	2.94E-05	0.259912	2593.228	1.353103	5.3696E-02
	MPA	8.364668	1.69E-06	0.343057	4972.814	1.103861	6.6668E-03
75°C	EO	8.379205	6.4E-06	0.308952	4989.473	1.207646	2.2820E-02
	WOA	8.387287	7.46E-06	0.314027	4664.953	1.221557	3.2939E-02
	PSO	8.424181	0.0021	-0.01934	1417.11	2.045836	1.8402E-01
	IPSO	8.415617	0.0001	0.213508	5000	1.498303	7.9559E-02

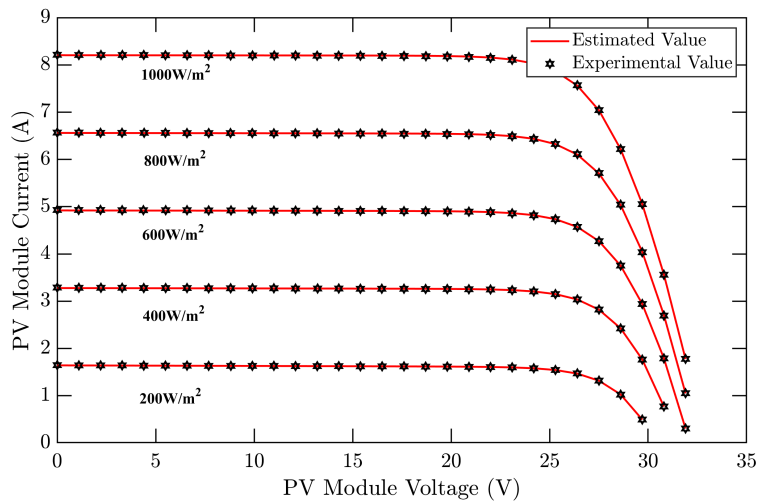
less RE, IAE<sub>i</sub>, and IAE<sub>p</sub>, as listed in Table 13 (for SDeM) and Table 15 (for DDeM). For SDeM of the Photowatt-PWP-201 PV module, the average values of RE, IAE<sub>i</sub>, and IAE<sub>p</sub> are 3.25E-04, 1.96E-03, and 2.07E-02, respectively, and for DDeM of the Photowatt-PWP-201 PV module, the average values of RE, IAE<sub>i</sub>, and IAE<sub>p</sub> are 3.26E-04, 1.96E-03,

and 2.07E-03, respectively. In order to visualize the I-V characteristics of both SDeM and DDeM of the Photowatt-PWP-201 PV module, the characteristic curves are illustrated in Fig. 9. From Fig. 9, it is observed that the experimental sample and estimated data are matching accurately. Therefore, from the above-all discussions, it is proved that

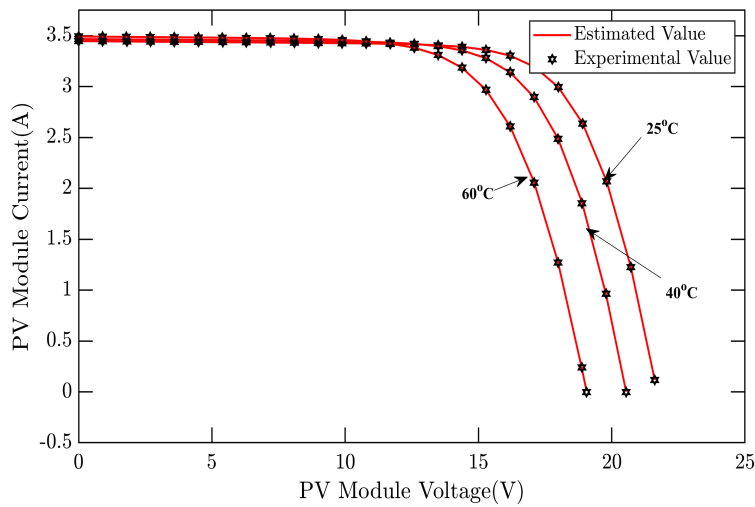
**TABLE 17.** Decision variables of the KC200GT PV module obtained by all algorithms under different irradiance conditions.

Condition	Algorithm	$I_p$ (A)	$I_{sd}$ (A)	$R_s$ ( $\Omega$ )	$R_p$ ( $\Omega$ )	$a$	RMSE
1000W/m <sup>2</sup>	CGBO	8.206257	3.91E-09	0.33611	2492.041	1.104013	5.1445E-03
	GBO	8.204752	3.24E-09	0.339289	2320.371	1.094464	5.6055E-03
	IMO	8.251763	2.01E-05	0.075865	2269.877	1.818535	9.2314E-02
	MPA	8.237377	6.35E-06	0.125199	4792.819	1.671877	7.6815E-02
	EO	8.226907	7.84E-07	0.209442	4997.609	1.460143	5.3061E-02
	WOA	8.259709	3.82E-05	0.037566	1223.715	1.910946	1.0189E-01
	PSO	8.301947	5.56E-05	0.016144	765.0737	1.968867	1.1277E-01
	IPSO	8.270254	0.0001	0	5000	2.072842	1.1627E-01
800W/m <sup>2</sup>	CGBO	6.562205	2.21E-09	0.342618	1534.004	1.074838	5.5503E-03
	GBO	6.555748	3.84E-09	0.331713	4988.073	1.102548	9.1070E-03
	IMO	6.605426	4.04E-05	0	4676.694	1.942802	9.4462E-02
	MPA	6.577328	7.4E-07	0.178713	4999.941	1.460498	4.9472E-02
	EO	6.577927	7.36E-07	0.180365	4958.47	1.460089	4.9442E-02
	WOA	6.616677	3.7E-05	0.007374	1097.671	1.929037	9.6883E-02
	PSO	6.564909	0.178296	-2.11715	4120.713	6.079291	2.1338E-01
	IPSO	6.566696	1.46E-07	0.23258	5000	1.327365	3.5642E-02
600W/m <sup>2</sup>	CGBO	4.921947	5.24E-09	0.331575	1581.609	1.12021	5.0603E-03
	GBO	4.920649	7.36E-09	0.324619	3549.742	1.138777	6.2228E-03
	IMO	4.956447	1.91E-05	0	4343.706	1.853594	6.6926E-02
	MPA	4.939686	2.63E-06	0.088329	4999.998	1.599185	4.4243E-02
	EO	4.932097	5.61E-07	0.16381	4996.83	1.445281	3.1859E-02
	WOA	4.99568	4.38E-06	0.012004	208.9506	1.657903	6.8755E-02
	PSO	5.087625	0.0001	0	1863.974	2.140382	1.4917E-01
	IPSO	4.997821	0.0001	0	5000	2.14622	1.2540E-01
400W/m <sup>2</sup>	CGBO	3.279337	2.94E-09	0.327414	1312.421	1.089004	3.8315E-03
	GBO	3.282883	2.45E-09	0.336103	1086.752	1.079609	2.7655E-03
	IMO	3.306257	1.07E-05	0	3809.161	1.801892	6.3662E-02
	MPA	3.281416	4.25E-07	0.026425	4999.983	1.424594	1.7366E-02
	EO	3.279753	4.28E-07	0	5000	1.423972	1.7835E-02
	WOA	3.316049	4.67E-06	0.093907	892.7713	1.694502	6.6284E-02
	PSO	3.315121	0.001202	-1.39541	1182.66	2.791425	5.9302E-02
	IPSO	3.335288	0.0001	0	5000	2.213591	1.1430E-01
200W/m <sup>2</sup>	CGBO	1.643011	1.82E-09	0.268534	827.3371	1.063041	1.1614E-03
	GBO	1.645863	9.6E-10	0.324039	707.9263	1.031613	3.5856E-03
	IMO	1.643025	1.42E-06	0	4999.829	1.581963	2.8717E-02
	MPA	1.631824	5.52E-09	0.224658	4314.544	1.123058	7.0862E-03
	EO	1.633029	2.96E-08	2.7E-08	4034.488	1.226212	6.8803E-03
	WOA	1.667573	2.6E-06	0.251213	621.0018	1.672866	4.8568E-02
	PSO	1.645423	0.001282	-4.00673	2019.802	2.934351	2.4848E-02
	IPSO	1.632365	2.52E-08	0.029768	5000	1.21576	7.0784E-03

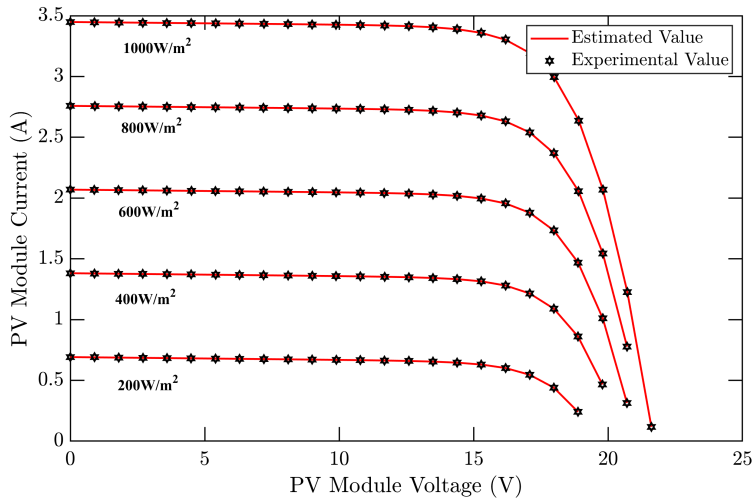
**FIGURE 10.** I-V curves of the KC200GT PV module under different temperature conditions.



**FIGURE 11.** I-V curves of the KC200GT PV module under different irradiance conditions.



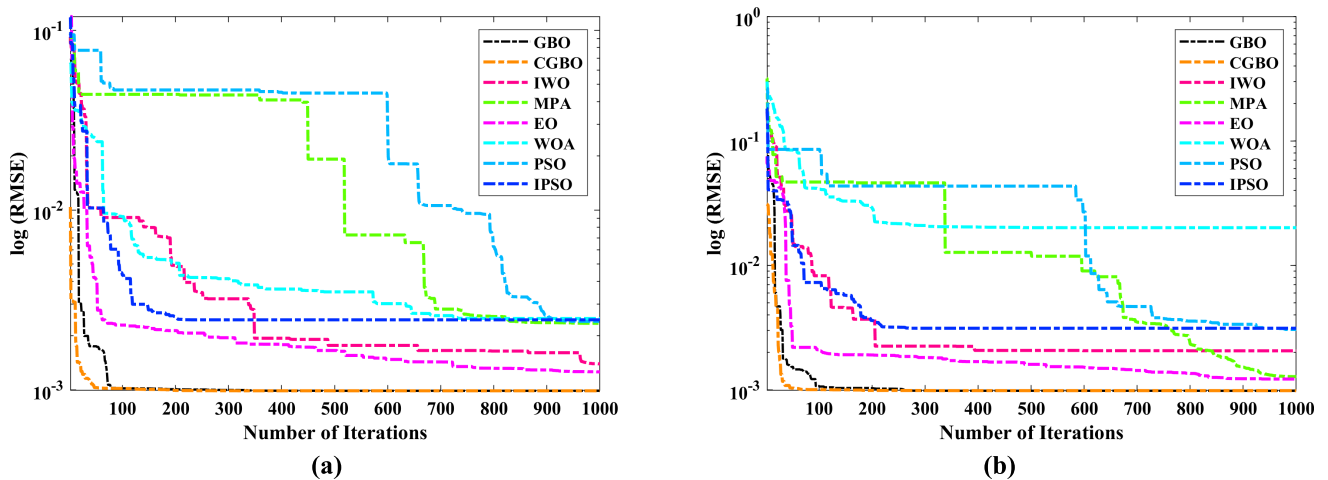
**FIGURE 12.** I-V curves of the SM55 PV module under different temperature conditions.



**FIGURE 13.** I-V curves of the SM55 PV module under different irradiance conditions.

**TABLE 18.** Decision variables of the SM55 PV module obtained by all algorithms under different temperature conditions.

Condition	Algorithm	$I_p$ (A)	$I_{sd}$ (A)	$R_s$ ( $\Omega$ )	$R_p$ ( $\Omega$ )	$a$	RMSE
25°C	CGBO	3.44892	1.75E-07	0.32913	514.5593	1.39748	1.1511E-03
	GBO	3.450104	1.71E-07	0.329147	483.9025	1.395753	1.3462E-03
	IMO	3.449672	1.97E-05	0.083349	4775.526	1.940924	2.8736E-02
	MPA	3.444941	5.42E-06	0.172233	4995.902	1.754257	1.9186E-02
	EO	3.441834	2.46E-06	0.219134	4999.92	1.656646	1.3948E-02
	WOA	3.458598	2.39E-05	0.085474	1638.162	1.973198	3.2145E-02
	PSO	3.48775	0.056572	-1.77634	2360.674	5.592765	1.1060E-01
	IPSO	3.469246	0.0001	0	5000	2.243364	4.7816E-02
50°C	CGBO	3.469137	1.15E-06	0.313096	533.0827	1.417839	3.7888E-03
	GBO	3.469138	1.15E-06	0.313096	533.0642	1.417839	3.7888E-03
	IMO	3.461189	5.18E-06	0.248916	4984.936	1.576211	9.8616E-03
	MPA	3.457553	2.31E-06	0.288398	4988.611	1.487183	6.3961E-03
	EO	3.463348	5.96E-06	0.235056	2315.23	1.592709	1.1069E-02
	WOA	3.504876	5.1E-06	0.292744	235.4211	1.57869	3.8414E-02
	PSO	3.441772	0.0001	0	1697.677	2.020512	4.8641E-02
	IPSO	3.477999	0.0001	0.035293	5000	2.019734	3.4810E-02
75°C	CGBO	3.494608	6.91E-06	0.318706	484.8835	1.405142	3.7804E-03
	GBO	3.494608	6.91E-06	0.318706	484.8841	1.405142	3.7804E-03
	IMO	3.490922	3.01E-05	0.241988	2005.047	1.581471	1.1094E-02
	MPA	3.492325	4.71E-05	0.209507	3527.971	1.643884	1.4560E-02
	EO	3.483392	1.28E-05	0.292914	5000	1.473605	5.9841E-03
	WOA	3.491212	2.76E-05	0.244386	1595.925	1.569386	1.0414E-02
	PSO	3.546993	0.030493	-0.93763	2200.143	3.845697	9.3246E-02
	IPSO	3.497096	0.0001	0.151457	5000	1.761419	2.1568E-02

**FIGURE 14.** Convergence curve of all algorithms for case study – 1; (a) SDeM, (b) DDeM.

the proposed CGBO algorithm is superior to all selected algorithms for the estimation of uncertain variables of the Photowatt-PWP-201 PV module. As similar to previous case studies, next to the CGBO algorithm, the performance of GBO is better than all other algorithms.

#### D. RESULTS BASED ON DATASHEET INFORMATION

The proposed CGBO algorithm is further examined for its feasibility study in solving the parameter estimation problem of large photovoltaic modules. Therefore, two commercial photovoltaic modules, namely KC200GT and SM55, are

**TABLE 19.** Decision variables of the SM55 PV module obtained by all algorithms under different irradiance conditions.

Condition	Algorithm	$I_p$ (A)	$I_{sd}$ (A)	$R_s$ ( $\Omega$ )	$R_p$ ( $\Omega$ )	$a$	RMSE
<b>1000W/m<sup>2</sup></b>	CGBO	3.450843	1.85E-07	0.325679	467.2506	1.402082	1.1455E-03
	GBO	3.450102	1.71E-07	0.329144	483.9341	1.395762	1.3862E-03
	IMO	3.451125	4.14E-05	0	4014.611	2.0655	3.5626E-02
	MPA	3.442461	1.72E-06	0.23545	2294.404	1.61604	1.1948E-02
	EO	3.441215	1.59E-06	0.237317	2681.823	1.607168	1.1482E-02
	WOA	3.458395	1.83E-05	0.128494	1722.303	1.93148	3.3802E-02
	PSO	3.510579	0.0001	0	2884.455	2.239416	6.0542E-02
	IPSO	3.469246	0.0001	0	5000	2.243364	4.7816E-02
	CGBO	2.760381	1.44E-07	0.337537	459.9301	1.381217	6.2858E-04
<b>800W/m<sup>2</sup></b>	GBO	2.760182	1.54E-07	0.334082	466.9101	1.386512	6.9484E-04
	IMO	2.753096	6.43E-06	0	1152.932	1.771062	1.3719E-02
	MPA	2.746824	1.16E-06	0.214625	4982.165	1.573558	6.9013E-03
	EO	2.748473	2.41E-06	0.150224	4995.679	1.653451	8.3174E-03
	WOA	2.767772	1.29E-06	0.185322	389.8211	1.584903	9.6171E-03
	PSO	2.763569	0.031841	-2.60995	2285.5	4.832971	5.7836E-02
	IPSO	2.777992	0.0001	0	5000	2.27199	5.0084E-02
	CGBO	2.070678	1.56E-07	0.331639	454.1206	1.387683	8.1329E-04
	GBO	2.070898	1.56E-07	0.330504	450.0581	1.387532	8.4395E-04
<b>600W/m<sup>2</sup></b>	IMO	2.059557	3.02E-06	0.087489	2234.832	1.689817	8.0084E-03
	MPA	2.066192	1.32E-05	0.000594	4999.805	1.899127	1.5851E-02
	EO	2.06195	5.55E-06	0.01569	2143.557	1.768602	9.6450E-03
	WOA	2.077546	1.41E-05	0.000601	685.564	1.912535	2.0428E-02
	PSO	2.0844	0.007219	-2.06002	2634.161	3.922552	4.2854E-02
	IPSO	2.087349	0.0001	0	5000	2.302545	4.9929E-02
	CGBO	1.382843	1E-07	0.396608	427.0765	1.352018	7.0761E-04
	GBO	1.382769	1.02E-07	0.395135	428.9034	1.353267	7.0839E-04
	IMO	1.374778	9.26E-06	0.004138	3334.181	1.867221	1.2773E-02
<b>400W/m<sup>2</sup></b>	MPA	1.368276	9.97E-07	0.218323	4512.39	1.569306	7.1086E-03
	EO	1.379147	1.22E-06	0.000632	562.4063	1.586405	3.2939E-03
	WOA	1.384036	3.86E-05	0.028004	2131.402	2.141395	2.6033E-02
	PSO	1.382059	0.001809	-2.78434	2833.463	3.203328	1.6134E-02
	IPSO	1.388003	0.0001	0	5000	2.36865	3.3922E-02
	CGBO	0.692014	1.31E-07	0.312406	438.0434	1.370901	5.2054E-04
	GBO	0.692014	1.31E-07	0.312406	438.0434	1.3709	5.2054E-04
	IMO	0.684536	1.61E-05	0	2695.774	2.010689	1.0784E-02
	MPA	0.683507	2.64E-06	0.00068	1294.244	1.704622	5.5661E-03
<b>200W/m<sup>2</sup></b>	EO	0.690719	3.63E-07	0	471.8901	1.464654	8.0926E-04
	WOA	0.690746	2.05E-05	0.018191	850.7806	2.070085	1.3114E-02
	PSO	0.680884	5.68E-05	-2.066	3850.407	2.221589	5.2428E-03
	IPSO	0.689602	0.0001	0	5000	2.462579	1.8500E-02

considered for further investigations. A total of 333 samples were collected from the datasheet at different irradiance and temperature levels. The KC200GT PV module is a multi-crystalline panel, and the SM55 PV module is a monocrystalline panel for industrial applications, which has 36 PV series-connected cells. The value of the  $I_{sc}$  finds the initial range of the  $I_p$ . The temperature coefficient of the short-circuit current  $\alpha$  has been taken from the datasheet (for SM55,  $\alpha = 1.2\text{mA}/^\circ\text{C}$  and for KC200GT,  $\alpha = 3.18\text{mA}/^\circ\text{C}$ ).

The  $I_{sc}$  is obtained using the datasheet information at standard test condition (STC), and it can be expressed in Eq. 41.

$$I_{sc}(T, G) = \frac{G}{G_{STC}} \times I_{sc-STC} + (T - T_{STC}) \alpha \quad (41)$$

where  $I_{sc-STC}$  denotes the  $I_{sc}$  at STC,  $G_{STC}$  and  $T_{STC}$  represent the irradiance and temperature at STC, and  $G$  and  $T$  denote the actual irradiance and temperature.

**TABLE 20.** Statistical results of all algorithms for case study-1.

Model	Algorithm	Min	Max	Mean	Median	STD	RT	Rank
SDeM	CGBO	<b>9.8602E-04</b>	<b>9.8602E-04</b>	<b>9.8602E-04</b>	<b>9.8602E-04</b>	<b>9.0751E-14</b>	<b>18.50</b>	<b>1</b>
	GBO	9.8602E-04	9.8602E-04	9.8602E-04	9.8602E-04	2.9876E-11	19.87	2
	IMO	1.3932E-03	3.0867E-03	2.1642E-03	2.0129E-03	8.5683E-04	17.46	4
	MPA	2.3408E-03	5.3061E-03	3.9218E-03	4.1184E-03	1.4924E-03	36.31	5
	EO	1.2571E-03	1.4846E-03	1.3823E-03	1.4050E-03	1.1544E-04	58.20	3
	WOA	2.4893E-03	5.3206E-03	3.8084E-03	3.6154E-03	1.4255E-03	35.96	8
	PSO	2.3988E-03	2.0754E-02	8.5794E-03	2.5854E-03	1.0544E-02	17.83	6
	IPSO	2.4480E-03	2.4480E-03	2.4480E-03	2.4480E-03	2.3764E-17	17.61	7
DDeM	CGBO	<b>9.8251E-04</b>	<b>9.8674E-04</b>	<b>9.8614E-04</b>	<b>9.8602E-04</b>	<b>5.4679E-07</b>	<b>18.38</b>	<b>1</b>
	GBO	9.8566E-04	1.0143E-03	9.9416E-04	9.8571E-04	1.7476E-05	19.80	2
	IMO	2.0593E-03	4.4541E-03	3.2603E-03	3.2677E-03	1.1974E-03	17.31	5
	MPA	1.2771E-03	2.8364E-03	1.9381E-03	1.7008E-03	8.0626E-04	35.65	4
	EO	1.2200E-03	1.5379E-03	1.4191E-03	1.4993E-03	1.7349E-04	58.63	3
	WOA	2.0085E-02	4.3403E-02	3.5524E-02	4.3084E-02	1.3371E-02	36.36	8
	PSO	3.0555E-03	2.9671E-02	1.2259E-02	4.0514E-03	1.5087E-02	17.31	6
	IPSO	3.1263E-03	3.1263E-03	3.1263E-03	3.1263E-03	2.9993E-17	17.38	7

**TABLE 21.** Statistical results of all algorithms for case study-2.

Model	Algorithm	Min	Max	Mean	Median	STD	RT	Rank
SDeM	CGBO	<b>2.523E-04</b>	<b>2.706E-04</b>	<b>2.619E-04</b>	<b>2.618E-04</b>	<b>1.623E-06</b>	<b>18.49</b>	<b>1</b>
	GBO	2.533E-04	2.567E-04	2.553E-04	2.560E-04	8.762E-06	21.04	2
	IMO	2.540E-02	2.543E-02	2.541E-02	2.540E-02	1.804E-05	17.19	5
	MPA	2.672E-04	6.914E-04	5.499E-04	6.911E-04	2.448E-04	35.53	3
	EO	2.540E-02	2.540E-02	2.540E-02	2.540E-02	4.249E-18	58.50	6
	WOA	1.296E-03	2.543E-02	1.738E-02	2.540E-02	1.393E-02	35.50	4
	PSO	1.918E-03	3.487E-02	1.402E-02	5.263E-03	1.814E-02	17.15	8
	IPSO	2.540E-02	3.611E-02	2.897E-02	2.540E-02	6.184E-03	17.04	7
DDeM	CGBO	<b>2.222E-04</b>	<b>2.602E-04</b>	<b>2.414E-04</b>	<b>2.417E-04</b>	<b>1.902E-05</b>	<b>17.07</b>	<b>1</b>
	GBO	2.325E-04	2.623E-04	2.513E-04	2.591E-04	1.636E-05	18.51	2
	IMO	6.683E-03	2.541E-02	1.917E-02	2.540E-02	1.081E-02	17.30	5
	MPA	6.858E-04	6.895E-04	6.881E-04	6.888E-04	1.987E-06	34.78	3
	EO	2.540E-02	2.540E-02	2.540E-02	2.540E-02	3.469E-18	56.74	6
	WOA	2.911E-03	2.540E-02	1.791E-02	2.540E-02	1.299E-02	35.07	4
	PSO	3.299E-03	3.430E-03	3.375E-03	3.398E-03	6.832E-05	16.92	7
	IPSO	2.151E+02	2.151E+02	2.151E+02	2.151E+02	0.000E+00	16.97	8

## 1) CASE STUDY-4

At different temperatures and irradiance, the parameter of the KC200GT PV module is obtained using all selected algorithms. The proposed CGBO and all other selected algorithms obtain the best parameters at different irradi-

ance (200 W/m<sup>2</sup>, 400 W/m<sup>2</sup>, 600 W/m<sup>2</sup>, 800 W/m<sup>2</sup>, and 1000 W/m<sup>2</sup>) with 25 °C constant temperature. Similarly, the parameters are obtained at different temperatures (25 °C, 50 °C, and 75 °C) with 1000 W/m<sup>2</sup> constant irradiance. Table 16 lists the optimized parameters of the KC200GT PV

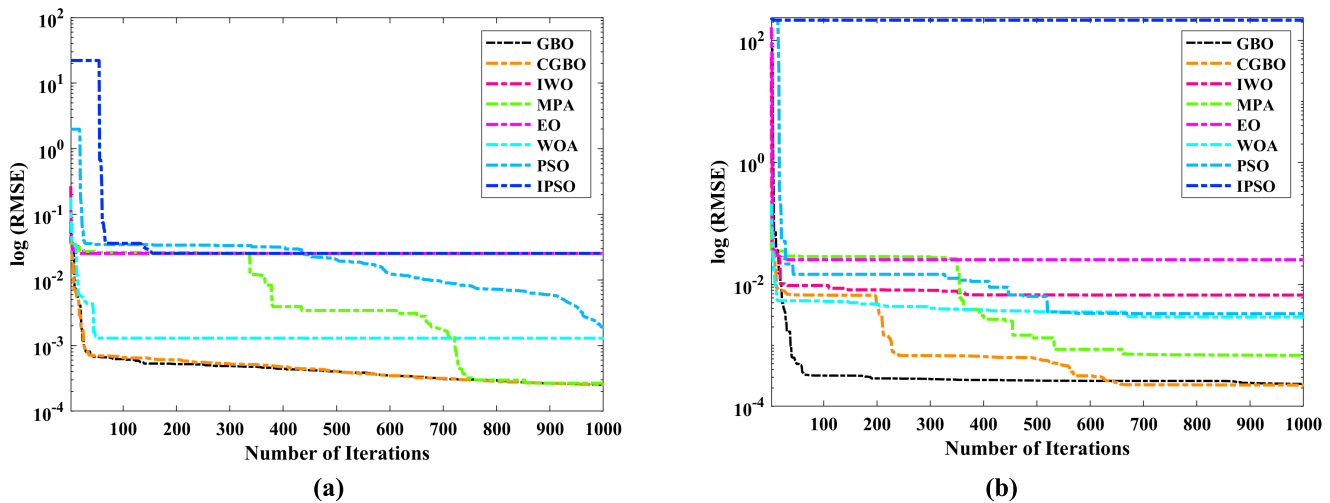


**FIGURE 15.** Convergence curve of all algorithms for case study – 2; (a) SDeM, (b) DDeM.

**TABLE 22.** Statistical results of all algorithms for case study-3.

Model	Algorithm	Min	Max	Mean	Median	STD	RT	Rank
SDeM	CGBO	2.425E-03	2.425E-03	2.425E-03	2.425E-03	2.058E-14	18.21	1
	GBO	2.425E-03	2.425E-03	2.425E-03	2.425E-03	2.254E-09	19.71	2
	IWO	2.759E-03	2.746E-01	9.476E-02	6.967E-03	1.557E-01	17.42	6
	MPA	2.593E-03	6.766E-03	3.991E-03	2.613E-03	2.404E-03	36.15	5
	EO	2.438E-03	2.608E-03	2.519E-03	2.512E-03	8.509E-05	58.09	3
	WOA	2.591E-03	7.334E-02	2.638E-02	3.219E-03	4.066E-02	35.60	4
	PSO	3.080E-03	7.297E-03	4.694E-03	3.705E-03	2.276E-03	17.43	8
	IPSO	2.608E-03	2.629E-03	2.615E-03	2.608E-03	1.222E-05	17.43	7
DDeM	CGBO	2.425E-03	2.425E-03	2.425E-03	2.425E-03	3.282E-08	18.15	1
	GBO	2.425E-03	2.447E-03	2.433E-03	2.427E-03	1.226E-05	19.16	2
	IWO	3.306E-03	2.745E-01	1.840E-01	2.743E-01	1.565E-01	17.16	7
	MPA	2.623E-03	2.688E-03	2.646E-03	2.628E-03	3.660E-05	36.61	5
	EO	2.469E-03	2.743E-01	9.306E-02	2.471E-03	1.569E-01	57.23	3
	WOA	8.997E-02	2.743E-01	1.542E-01	9.841E-02	1.041E-01	35.34	8
	PSO	3.207E-03	5.176E-02	2.232E-02	1.199E-02	2.587E-02	17.24	6
	IPSO	2.608E-03	1.062E+01	5.121E+00	4.738E+00	5.320E+00	17.62	4

module under different temperature conditions by all selected algorithms. For all temperature conditions, the proposed CGBO algorithm obtains less RMSE value, i.e., 6.4518E-03 (for 25°C), 2.7581E-03 (for 50°C), and 4.4558E-03 (for 75°C) than all other algorithms. Similarly, Table 17 lists the optimized parameters under different irradiance condi-

tions by all selected algorithms. For all irradiance conditions, the proposed CGBO algorithm obtains less RMSE value, i.e., 1.5445E-03 (for 1000W/m<sup>2</sup>), 5.5503E-03 (for 800W/m<sup>2</sup>), 5.0603E-03 (for 600W/m<sup>2</sup>), 3.8315E-03 (for 400W/m<sup>2</sup>), and 1.1614E-03 (for 200W/m<sup>2</sup>) than all other algorithms. Further, it is also observed that the PSO algorithm

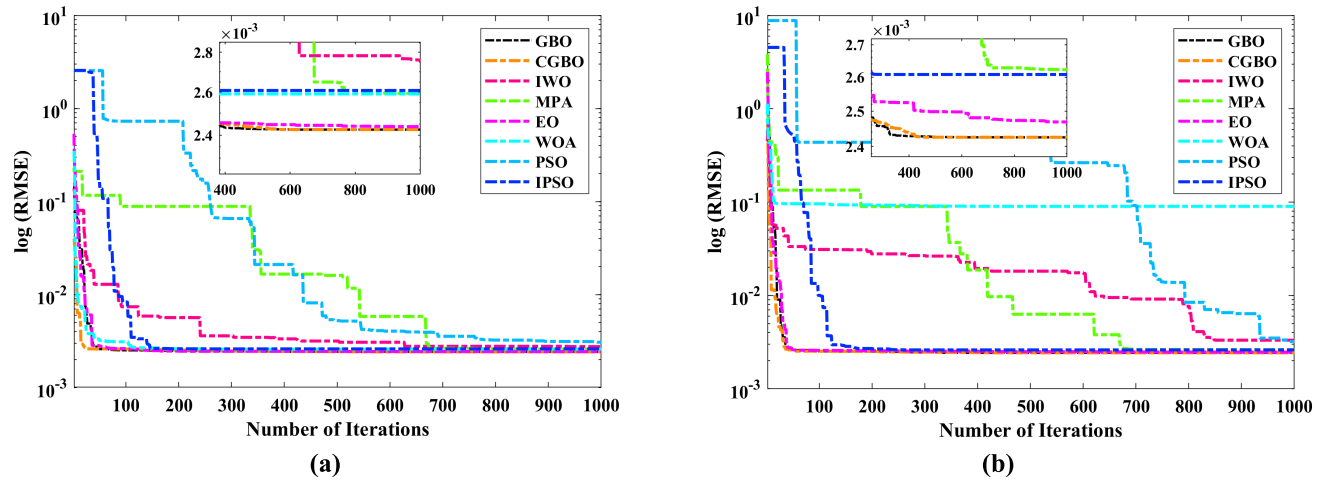


**FIGURE 16.** Convergence curve of all algorithms for case study – 3; (a) SDeM, (b) DDeM.

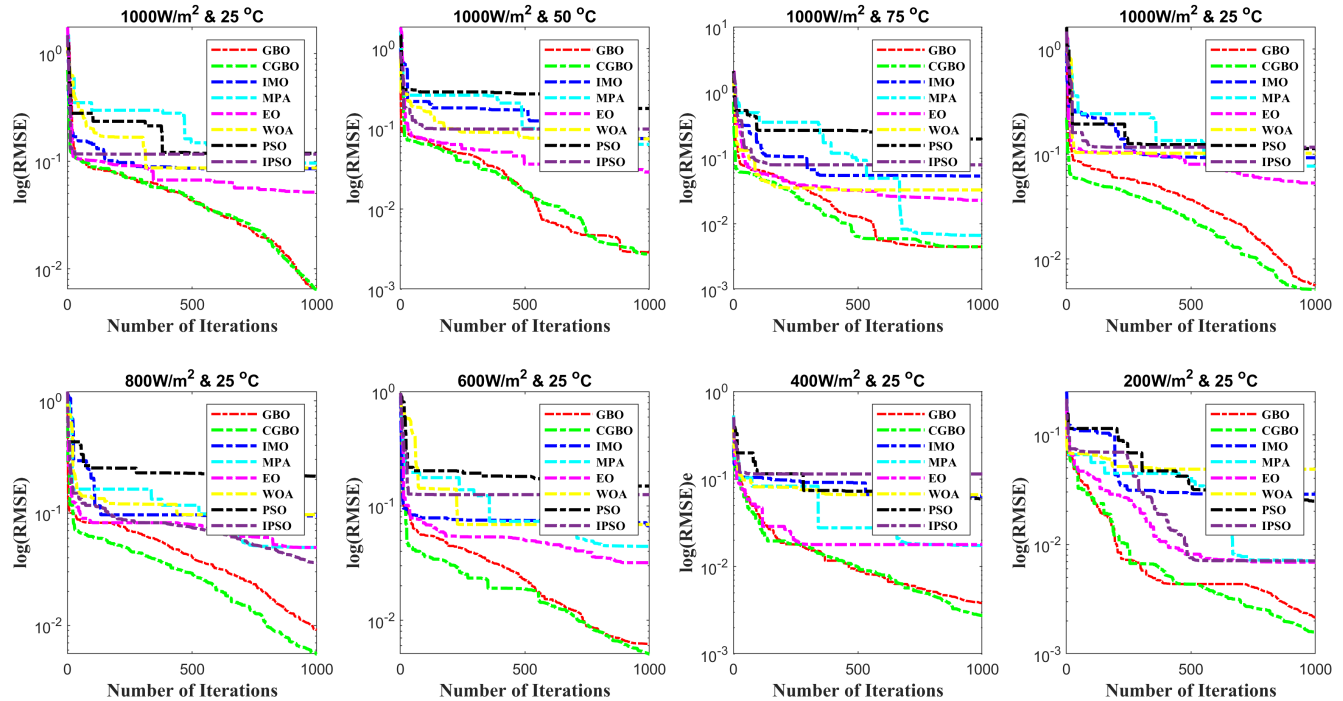


**FIGURE 17.** Convergence curve of all algorithms for case study-4.

is searching for the solution outside the boundary, and therefore, an effective constraint handling mechanism is required to bring the particles inside the boundary. Also, the IPSO algorithm is stuck at local optima, and therefore, the solution accuracy is very poor. Therefore, it is decided not to select the PSO and IPSO algorithm for parameter estimation problems. Figs. 10–11 demonstrates the accuracy of fitting the estimated parameters with the experimental parameters under different temperatures (with constant irradiance) and different irradiance (with constant temperature), which proves further the effectiveness of the proposed CGBO algorithm. Therefore, based on RMSE values and the I-V curve fitness, it is proved that the proposed CGBO algorithm is superior to all selected algorithms. Next to the CGBO algorithm, the basic variant

of the GBO algorithm is performing better than all other algorithms.

## 2) CASE STUDY-5

As similar to case study-4, at different temperatures and irradiance, the parameter of the SM55 PV module is obtained using all selected algorithms. The proposed CGBO and all other selected algorithms obtain the best parameters at different irradiance ( $200 \text{ W/m}^2$ ,  $400 \text{ W/m}^2$ ,  $600 \text{ W/m}^2$ ,  $800 \text{ W/m}^2$ , and  $1000 \text{ W/m}^2$ ) with  $25^\circ\text{C}$  constant temperature. Similarly, the parameters are obtained at different temperatures ( $25^\circ\text{C}$ ,  $40^\circ\text{C}$ , and  $60^\circ\text{C}$ ) with  $1000 \text{ W/m}^2$  constant irradiance. The experimental samples are listed in the Appendix (refer to

**TABLE 23.** Statistical results of all algorithms for case study-4.

Testing Conditions	Algorithm	Min	Max	Mean	Median	STD	RT	Rank
1000W/m <sup>2</sup> & 25 °C	GBO	0.006700795	0.010820369	0.008197025	0.00706991	0.002279367	22.13020833	2
	<b>CGBO</b>	<b>0.006451774</b>	<b>0.009448355</b>	<b>0.007801535</b>	<b>0.007504476</b>	<b>0.001520216</b>	<b>20.625</b>	<b>1</b>
	IMO	0.085144159	0.12176692	0.103853683	0.104649971	0.018324361	19.79166667	4
	MPA	0.096063937	0.102349168	0.098395893	0.096774576	0.003442025	41.05208333	6
	EO	0.051490407	0.104239662	0.072398055	0.061464097	0.028022929	66.21875	3
	WOA	0.086519109	0.188526005	0.131120877	0.118317517	0.052194791	38.24479167	5
	PSO	0.118432444	0.277125938	0.17269548	0.122528057	0.09046261	19.8125	8
	IPSO	0.116270097	0.116270097	0.116270097	0.116270097	2.4037E-17	19.828125	7
1000W/m <sup>2</sup> & 50 °C	GBO	0.002886922	0.004742437	0.004121681	0.004735683	0.001069338	19.46875	2
	<b>CGBO</b>	<b>0.002758132</b>	<b>0.004570079</b>	<b>0.003500875</b>	<b>0.003174415</b>	<b>0.000949063</b>	<b>21.07291667</b>	<b>1</b>
	IMO	0.075537799	0.099255921	0.090035578	0.095313014	0.012709281	19.359375	6
	MPA	0.06398826	0.095264179	0.078824423	0.07722083	0.015699503	39.40625	4
	EO	0.028886839	0.041118305	0.036729954	0.040184718	0.006808358	63.671875	3
	WOA	0.074917949	0.144070647	0.098762805	0.077299819	0.039255811	37.50520833	5
	PSO	0.179071603	0.275551655	0.230888473	0.238042159	0.048636216	19.234375	8
	IPSO	0.099118392	0.099118392	0.099118392	0.099118392	6.50926E-17	19.19791667	7
1000W/m <sup>2</sup> & 75 °C	GBO	0.004475767	0.004535679	0.004511463	0.004522944	3.1563E-05	20.296875	2
	<b>CGBO</b>	<b>0.00447293</b>	<b>0.004473121</b>	<b>0.004472994</b>	<b>0.004472931</b>	<b>1.09838E-07</b>	<b>18.57291667</b>	<b>1</b>
	IMO	0.053696378	0.120502713	0.079143371	0.063231023	0.036134108	19.41666667	6
	MPA	0.006666815	0.063920964	0.038634884	0.045316873	0.029206097	37.55208333	3
	EO	0.022820145	0.028790142	0.024831671	0.022884726	0.003428289	60.94791667	4
	WOA	0.032938865	0.381157138	0.15027263	0.036721887	0.199960795	36.59895833	5
	PSO	0.184018831	0.315947118	0.260237725	0.280747228	0.0683136	18.296875	8
	IPSO	0.079558793	0.079558793	0.079558793	0.079558793	7.14403E-17	18.390625	7
1000W/m <sup>2</sup> & 25 °C	GBO	0.005605516	0.006966925	0.006319534	0.00638616	0.000683146	21.23958333	2
	<b>CGBO</b>	<b>0.005144489</b>	<b>0.008291355</b>	<b>0.006958443</b>	<b>0.007439485</b>	<b>0.001627649</b>	<b>20.19791667</b>	<b>1</b>
	IMO	0.092313844	0.105156104	0.099233653	0.100231009	0.006478962	19.32291667	5
	MPA	0.07681453	0.100529791	0.089459057	0.09103285	0.011935704	39.109375	4
	EO	0.053060861	0.057898072	0.054700862	0.053143654	0.002769174	64.19791667	3
	WOA	0.10189212	0.15551717	0.12105611	0.105759042	0.029906717	37.91666667	6
	PSO	0.112774207	0.268983675	0.194142006	0.200668137	0.078308954	19.53645833	8
	IPSO	0.116270097	0.116270097	0.116270097	0.116270097	2.19427E-17	19.640625	7
800W/m <sup>2</sup> & 25 °C	GBO	0.009107025	0.010778707	0.010206402	0.010733475	0.000952357	20.03645833	2
	<b>CGBO</b>	<b>0.00555034</b>	<b>0.007750835</b>	<b>0.006885941</b>	<b>0.007356649</b>	<b>0.001173336</b>	<b>21.119791667</b>	<b>1</b>
	IMO	0.094461522	0.108495079	0.101618983	0.10190035	0.007021008	19.515625	6
	MPA	0.049472319	0.091393829	0.065612398	0.055971045	0.02256258	38.97395833	5
	EO	0.049441869	0.082144029	0.062432577	0.055711834	0.017356098	65.11458333	4
	WOA	0.096882729	0.108305834	0.103743104	0.106040751	0.006048241	37.31770833	7
	PSO	0.21337664	0.237402716	0.226276025	0.228048719	0.012110735	19.33333333	8
	IPSO	0.035641922	0.127252537	0.096715665	0.127252537	0.052891413	19.27083333	3
600W/m <sup>2</sup> & 25 °C	GBO	0.006222822	0.006672719	0.006497907	0.006598179	0.000241128	19.60416667	2
	<b>CGBO</b>	<b>0.005060282</b>	<b>0.006282261</b>	<b>0.005847229</b>	<b>0.006199143</b>	<b>0.000682782</b>	<b>21.22916667</b>	<b>1</b>
	IMO	0.066926288	0.082333624	0.073053771	0.069901401	0.008173101	19.375	5
	MPA	0.044243355	0.056843871	0.051303249	0.052822521	0.006436179	39.109375	4
	EO	0.031858673	0.054729144	0.040138835	0.033828687	0.012673913	64.08854167	3
	WOA	0.068755047	0.166632531	0.113084839	0.103866938	0.04958556	37.46875	6
	PSO	0.149173709	0.195133261	0.176674004	0.185715042	0.024277054	19.27083333	8
	IPSO	0.125402538	0.125402538	0.125402538	0.125402538	1.96262E-17	19.375	7

**TABLE 23.** (Continued.) Statistical results of all algorithms for case study-4.

400W/m <sup>2</sup> & 25 °C	GBO	0.003831526	0.006551495	0.004893316	0.004296926	0.001454757	21.09375	2
	<b>CGBO</b>	<b>0.002765479</b>	<b>0.005338902</b>	<b>0.004111444</b>	<b>0.004229952</b>	<b>0.001290798</b>	<b>19.33854167</b>	<b>1</b>
	IMO	0.063661904	0.08984142	0.074510679	0.070028712	0.013653124	19.125	5
	MPA	0.017366297	0.060785398	0.031902332	0.0175553	0.025013648	38.72395833	3
	EO	0.017835253	0.01783533	0.017835279	0.017835253	4.42532E-08	64.83333333	4
	WOA	0.066283597	0.089549545	0.075277875	0.070000484	0.012498569	37.11458333	6
	PSO	0.059302017	0.066654955	0.063493439	0.064523345	0.003783114	19.07291667	8
	IPSO	0.114302078	0.114302078	0.114302078	1.38778E-17	19.15104167		7
200W/m <sup>2</sup> & 25 °C	GBO	0.002161416	0.003240864	0.002529284	0.002185572	0.000616365	20.875	2
	<b>CGBO</b>	<b>0.001585565</b>	<b>0.002064613</b>	<b>0.001826568</b>	<b>0.001829526</b>	<b>0.000239538</b>	<b>19.52083333</b>	<b>1</b>
	IMO	0.028716803	0.061901823	0.050262775	0.060169699	0.018679447	19.58854167	6
	MPA	0.007086216	0.026529571	0.015021362	0.011448299	0.01020226	38.265625	5
	EO	0.006880321	0.00710741	0.007031712	0.007107405	0.000131108	63.39583333	3
	WOA	0.048567526	0.057385457	0.054383347	0.057197045	0.00503753	37.02604167	7
	PSO	0.024848117	0.033434935	0.028130441	0.026108271	0.004636835	18.89583333	8
	IPSO	0.007078424	0.069382175	0.048614258	0.069382175	0.035971088	19.11979167	4

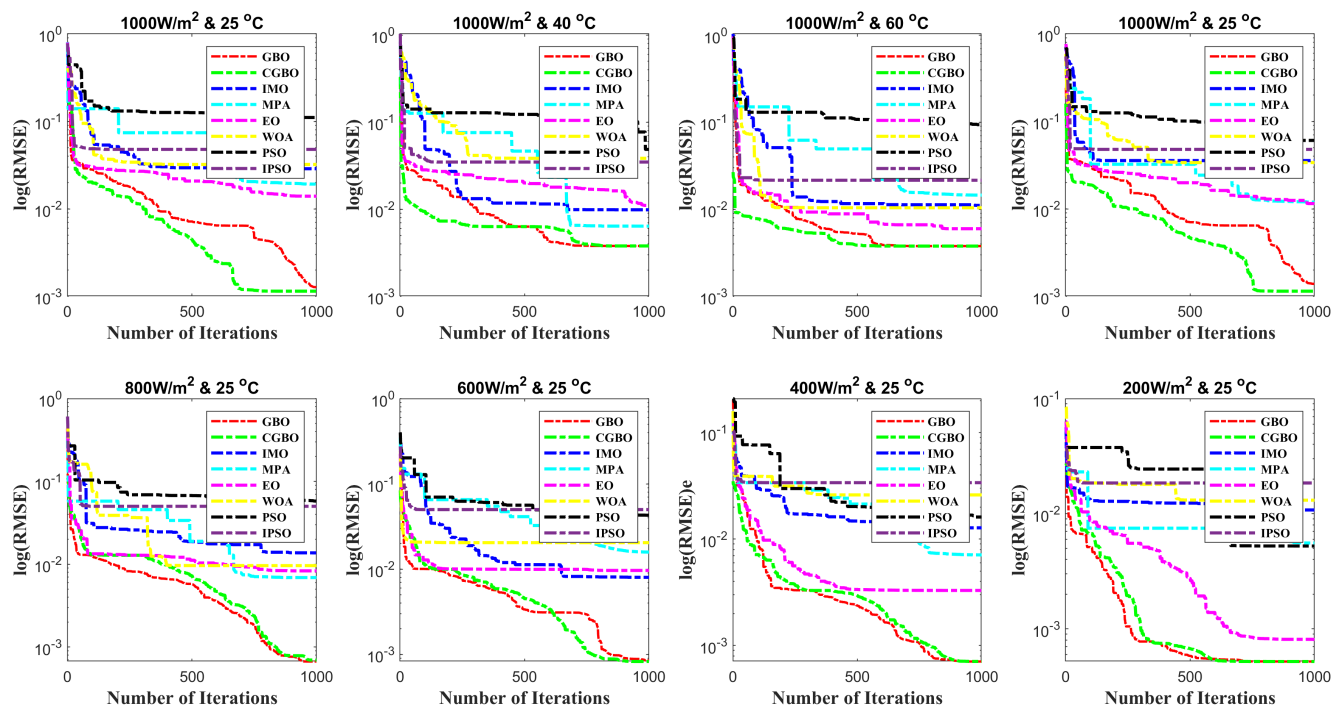
**FIGURE 18.** Convergence curve of all algorithms for case study-5.

Table 26 and Table 27). Table 18 lists the optimized parameters of the KC200GT PV module under different temperature conditions by all selected algorithms. For all temperature conditions, the GBO and the proposed CGBO algorithm obtains less RMSE values, i.e., 1.1511E-03 (for 25°C), 3.7888E-03 (for 40°C), and 3.7804E-03 (for 60°C) than all other algorithms. Similarly, Table 19 lists the optimized parameters under different irradiance conditions by all selected algorithms. For all irradiance conditions, the proposed CGBO

algorithm obtains less RMSE value, i.e., 1.1455E-03 (for 1000W/m<sup>2</sup>), 6.2858E-03 (for 800W/m<sup>2</sup>), 8.1329E-03 (for 600W/m<sup>2</sup>), 7.0761E-03 (for 400W/m<sup>2</sup>), and 5.2054E-03 (for 200W/m<sup>2</sup>) than all other algorithms. Like previous case studies, the PSO algorithm is searching for the solution outside the boundary. Therefore, it is decided not to select the PSO algorithm without a constraint handling mechanism for parameter estimation problems. Figs. 12-13 demonstrates the accuracy of fitting the estimated parameters with the experimental

**TABLE 24.** Statistical results of all algorithms for case study-5.

Testing Conditions	Algorithm	Min	Max	Mean	Median	STD	RT	Rank
1000W/m <sup>2</sup> & 25 °C	GBO	0.001146	0.001402	0.001231	0.001146	0.000148	22.03125	2
	<b>CGBO</b>	<b>0.001251</b>	<b>0.003888</b>	<b>0.002295</b>	<b>0.001745</b>	<b>0.001402</b>	<b>20.22396</b>	<b>1</b>
	IMO	0.028736	0.036087	0.03355	0.035826	0.004171	19.69792	5
	MPA	0.019186	0.037858	0.031113	0.036296	0.010359	39.83854	4
	EO	0.013948	0.035555	0.028353	0.035555	0.012475	64.36979	3
	WOA	0.032145	0.062379	0.043954	0.037336	0.016167	39.33854	6
	PSO	0.110598	0.135467	0.122545	0.12157	0.012463	19.20313	8
	IPSO	0.047816	0.047816	0.047816	0.047816	4.91E-18	19.3125	7
1000W/m <sup>2</sup> & 40 °C	GBO	0.003789	0.004242	0.003962	0.003855	0.000245	20.39583	2
	<b>CGBO</b>	<b>0.003789</b>	<b>0.003789</b>	<b>0.003789</b>	<b>0.003789</b>	<b>1.41E-08</b>	<b>18.47917</b>	<b>1</b>
	IMO	0.009862	0.034087	0.025455	0.032417	0.01353	18.08333	4
	MPA	0.006396	0.03333	0.015692	0.007351	0.015282	37.20313	3
	EO	0.011069	0.037672	0.021183	0.014807	0.014402	60.06771	5
	WOA	0.038414	0.059279	0.047238	0.04402	0.010798	36.5	6
	PSO	0.048641	0.136163	0.09278	0.093536	0.043766	17.96875	8
	IPSO	0.03481	0.03481	0.03481	0.03481	4.47E-17	18.94271	7
1000W/m <sup>2</sup> & 60 °C	GBO	0.00378	0.00378	0.00378	0.00378	4.93E-14	20.21875	2
	<b>CGBO</b>	<b>0.00378</b>	<b>0.00378</b>	<b>0.00378</b>	<b>0.00378</b>	<b>5.33E-08</b>	<b>18.26563</b>	<b>1</b>
	IMO	0.011094	0.022232	0.014993	0.011653	0.006275	17.82292	5
	MPA	0.01456	0.019711	0.017915	0.019475	0.002908	36.00521	6
	EO	0.005984	0.007069	0.006495	0.006431	0.000545	59.20313	3
	WOA	0.010414	0.018127	0.014388	0.014622	0.003862	36.10938	4
	PSO	0.093246	0.133077	0.112346	0.110716	0.019965	17.67188	8
	IPSO	0.021568	0.021568	0.021568	0.021568	6.82E-17	17.80208	7
1000W/m <sup>2</sup> & 25 °C	GBO	0.001386	0.005033	0.002609	0.001408	0.0021	20.11458	2
	<b>CGBO</b>	<b>0.001146</b>	<b>0.002453</b>	<b>0.001582</b>	<b>0.001147</b>	<b>0.000754</b>	<b>19.25</b>	<b>1</b>
	IMO	0.035626	0.04268	0.039529	0.040281	0.003587	18.19792	6
	MPA	0.011948	0.035081	0.021919	0.018729	0.011892	37.09375	4
	EO	0.011482	0.014938	0.013696	0.014669	0.001923	60.75521	3
	WOA	0.033802	0.044525	0.040571	0.043386	0.00589	36.73438	5
	PSO	0.060542	0.121688	0.098409	0.112998	0.033081	18.36979	8
	IPSO	0.047816	0.047816	0.047816	0.047816	6.94E-18	18.5	7
800W/m <sup>2</sup> & 25 °C	GBO	0.000695	0.00297	0.001437	0.000673	0.001327	20.50521	2
	<b>CGBO</b>	<b>0.000669</b>	<b>0.00167</b>	<b>0.001066</b>	<b>0.000834</b>	<b>0.000528</b>	<b>18.53125</b>	<b>1</b>
	IMO	0.013719	0.039031	0.027604	0.030062	0.012833	18.17188	6
	MPA	0.006901	0.016884	0.01257	0.013925	0.005127	36.375	3
	EO	0.008317	0.012831	0.009955	0.008715	0.002499	59.96354	4
	WOA	0.009617	0.059781	0.030551	0.022255	0.026091	36.45313	5
	PSO	0.057836	0.075206	0.065431	0.063252	0.008888	18.07813	8
	IPSO	0.050084	0.050084	0.050084	0.050084	1.77E-17	19.10417	7
600W/m <sup>2</sup> & 25 °C	GBO	0.000843	0.001262	0.001013	0.000933	0.00022	19.80208	2
	<b>CGBO</b>	<b>0.000824</b>	<b>0.001042</b>	<b>0.000897</b>	<b>0.000824</b>	<b>0.000126</b>	<b>18.16667</b>	<b>1</b>
	IMO	0.008008	0.033861	0.021869	0.023738	0.013027	17.97396	3
	MPA	0.015851	0.01749	0.016438	0.015973	0.000913	36.26563	5
	EO	0.009645	0.010041	0.009875	0.009938	0.000206	59.91146	4
	WOA	0.020428	0.073122	0.04454	0.040071	0.02663	36.26563	6
	PSO	0.042854	0.066427	0.057351	0.06277	0.012687	18.02083	8
	IPSO	0.049929	0.049929	0.049929	0.049929	4.91E-18	17.98438	7

**TABLE 24.** (Continued.) Statistical results of all algorithms for case study-5.

400W/m <sup>2</sup> & 25 °C	GBO	0.000708	0.000781	0.000732	0.000708	4.21E-05	19.78646	2
	<b>CGBO</b>	<b>0.000708</b>	<b>0.00071</b>	<b>0.000709</b>	<b>0.000709</b>	<b>7.13E-07</b>	<b>18.3125</b>	<b>1</b>
	IMO	0.012773	0.026249	0.019061	0.018161	0.006783	17.97396	5
	MPA	0.007109	0.016318	0.012924	0.015344	0.005059	36.26042	4
	EO	0.003294	0.003323	0.003305	0.003298	1.56E-05	59.24479	3
	WOA	0.026033	0.03236	0.029726	0.030787	0.003294	36.77604	6
	PSO	0.016134	0.027311	0.022602	0.02436	0.005792	18.92708	8
	IPSO	0.033922	0.033922	0.033922	0.033922	1.77E-17	19.26042	7
200W/m <sup>2</sup> & 25 °C	GBO	0.000521	0.000521	0.000521	0.000521	5.66E-08	20.26563	2
	<b>CGBO</b>	<b>0.000521</b>	<b>0.000522</b>	<b>0.000521</b>	<b>0.000521</b>	<b>9.14E-07</b>	<b>18.72917</b>	<b>1</b>
	IMO	0.010784	0.015629	0.013323	0.013554	0.002431	18.02083	5
	MPA	0.005566	0.010033	0.00768	0.007441	0.002243	36.38542	4
	EO	0.000809	0.000922	0.000875	0.000892	5.85E-05	61.54688	3
	WOA	0.013114	0.014804	0.014126	0.01446	0.000893	37.40104	6
	PSO	0.005243	0.011095	0.007698	0.006757	0.003037	18.26042	8
	IPSO	0.0185	0.0185	0.0185	0.0185	4.91E-18	18.03646	7

**TABLE 25.** A brief comparison of various algorithms using specific parameters.

S. No.	Algorithm	Ref.	Control Variables	Benchmark functions	Remarks
1	Genetic Algorithm (GA)	[18]	N=50, $m_{max}=200$ , $P_c=0.95$ , $P_m=0.001$	Six unconstrained problems	First evolutionary computation algorithm
2	Particle Swarm Optimization (PSO)	[20]	N=50, $m_{max}=500$ , $w_{Max}=0.9$ , $w_{Min}=0.6$ , $c_1$ and $c_2=2$	Unconstrained problems	Tested for many real-world problems
3	Differential Evolutionary (DE)	[25]	N=40, $m_{max}=200$ , $P_{cr}=0.2$	Eight unconstrained problems	Tested for real-world constrained problems
4	Grey Wolf Optimizer (GWO)	[31]	N=30, $m_{max}=500$ , $a=2$	CEC2005 special session test functions	Tested for constrained real-world problems
5	Whale Optimizer Algorithm (WOA)	[32]	N=30, $m_{max}=500$ , $a=[2,0]$	CEC2006 test functions	Tested for constrained real-world problems
6	Salp Swarm Algorithm (SSA)	[34]	N=30, $m_{max}=500$	CEC2017 test functions	Tested for single and multi-objective problems
7	Teaching-Learning Optimization (TLBO)	[38]	N=100, $m_{max}=500$	CEC2005 benchmark test functions	Real-world problems are not tested
8	JAYA	[35]	N=100, $m_{max}=500$	CEC2006 benchmark test functions	Real-world problems are not tested
9	Marine Predator Algorithm (MPA)	[46]	N=30, $m_{max}=500$ , $P=0.5$ , $v=0.1$	CEC2017 test functions	Tested for 3 constrained RW problems
10	Equilibrium Optimizer (EO)	[47]	N=30, $m_{max}=500$ , $GP=0.5$	CEC2017 test functions including	Tested for constrained real-world problems
11	Intelligent Water-drop Optimization (IWO)	[48]	N=50, $m_{max}=500$	Not tested	Tested for Knapsack problem and travelling salesman problem
12	RAO	[69]	N=100, $m_{max}=500$	CEC2006 benchmark test functions	Real-world problems are not tested

parameters under different temperatures (with constant irradiance) and different irradiance (with constant temperature), which proves further the effectiveness of the proposed CGBO algorithm. Therefore, based on RMSE values and the I-V curve fitness, it is proved that the proposed CGBO algorithm is superior to all selected algorithms. Next to the CGBO algorithm, the basic variant of the GBO algorithm is performing better than all other algorithms.

## E. PERFORMANCE ANALYSIS

The performance of the proposed CGBO algorithm is further verified by analyzing the statistical data for the first three case studies. The statistical data, such as Min, Max, Mean, Median, STD, and RT, are obtained for all selected algorithms. The statistical data based on mean RMSE values are compared with other selected algorithms, and the rank is provided based on minimum RMSE values.

**TABLE 26.** SM55 - experimental data - different irradiance at constant temperature.

200 W/m <sup>2</sup>		400 W/m <sup>2</sup>		600 W/m <sup>2</sup>		800 W/m <sup>2</sup>		1000 W/m <sup>2</sup>	
V	I	V	I	V	I	V	I	V	I
0.00	0.69	0.00	1.38	0.00	2.07	0.00	2.76	0.00	3.45
0.66	0.69	0.50	1.38	0.65	2.07	0.51	2.76	0.70	3.45
1.35	0.69	1.05	1.38	1.13	2.07	1.04	2.76	1.41	3.45
2.17	0.68	1.78	1.38	1.74	2.07	1.58	2.75	1.94	3.45
2.95	0.68	2.58	1.37	2.40	2.06	2.17	2.75	2.50	3.45
3.66	0.68	3.24	1.37	3.24	2.06	2.90	2.75	3.08	3.44
4.42	0.67	3.86	1.37	3.85	2.06	3.52	2.75	4.47	3.44
5.10	0.67	4.50	1.36	4.26	2.06	4.24	2.75	5.02	3.44
5.67	0.67	5.24	1.36	4.74	2.06	4.81	2.75	6.13	3.44
6.24	0.67	5.98	1.36	5.26	2.06	5.39	2.75	7.26	3.44
6.68	0.67	6.81	1.36	5.79	2.06	6.20	2.74	8.30	3.44
7.07	0.67	7.40	1.36	6.32	2.05	6.85	2.74	8.87	3.43
7.54	0.67	8.09	1.35	6.78	2.05	7.54	2.74	9.44	3.43
8.03	0.66	8.60	1.36	7.40	2.05	8.26	2.75	10.00	3.43
8.55	0.66	9.25	1.35	7.95	2.05	9.10	2.74	10.57	3.43
9.07	0.66	9.89	1.35	8.61	2.05	9.77	2.74	11.72	3.43
9.67	0.66	10.58	1.35	9.22	2.05	10.39	2.74	12.58	3.43
10.17	0.66	11.29	1.35	9.77	2.05	11.20	2.74	12.94	3.43
10.65	0.66	12.06	1.34	10.29	2.04	11.93	2.74	13.80	3.41
11.20	0.65	12.74	1.35	10.82	2.04	12.31	2.73	14.21	3.41
11.71	0.65	13.44	1.35	11.29	2.04	12.72	2.73	14.67	3.39
12.12	0.65	14.13	1.34	11.86	2.04	13.07	2.73	15.12	3.38
12.63	0.65	14.69	1.33	12.40	2.04	13.46	2.73	16.35	3.30
13.10	0.65	15.00	1.33	12.90	2.04	14.26	2.71	16.72	3.27
13.61	0.65	15.39	1.32	13.67	2.03	15.07	2.69	17.79	3.08
14.12	0.65	15.80	1.30	14.36	2.03	15.76	2.67	18.34	2.91
14.76	0.64	16.18	1.29	14.99	2.01	16.63	2.61	18.77	2.73
15.33	0.64	16.51	1.27	15.75	1.99	17.10	2.56	19.02	2.58
15.94	0.62	17.16	1.23	16.14	1.97	17.72	2.46	19.44	2.28
16.20	0.61	17.76	1.16	16.50	1.95	18.16	2.36	19.68	2.06
16.73	0.59	18.03	1.12	17.15	1.89	18.60	2.21	19.86	1.92
17.20	0.55	18.55	1.00	17.75	1.81	19.08	1.97	20.06	1.72
17.70	0.51	18.98	0.86	18.56	1.61	19.53	1.66	20.66	1.13
18.16	0.45	19.56	0.59	19.51	1.15	20.01	1.29	20.85	0.92
18.73	0.33	20.08	0.28	20.16	0.70	20.58	0.80	21.62	0.00
19.69	0.00	20.52	0.00	21.02	0.00	21.33	0.00	-	-

For case study-1, all the statistical data are listed in Table 20. From Table 20, it is observed that both GBO and CGBO algorithms produce the same RMSE values; however, the rank is provided based on the STD and RT values. Out of eight algorithms, the IMO algorithm holds the first position in terms of RT, followed by IPSO, PSO, CGBO, GBO, WOA, MPA, and EO. However, based on reliability (minimum STD) and Min values, the proposed CGBO holds the first position, followed by GBO, EO, IMO, MPA, IPSO, PSO. To visualize the convergence behavior of all algorithms, the convergence curves for SDeM and DDeM are illustrated in Fig. 14. From Fig. 14, it is observed that the convergence speed of the proposed CGBO algorithm is high compared to all other algorithms.

For case study-2, all the statistical data are listed in Table 21. Out of eight algorithms, the IPSO algorithm holds the first position in terms of RT, followed by PSO, IMO,

CGBO, GBO, MPA, WOA, and EO. However, based on reliability (minimum STD) and Min values, the proposed CGBO holds the first position, followed by GBO, MPA, WOA, EO, IMO, PSO, and IPSO. Both PSO and IPSO fail to find the global optima as per the earlier discussions. To visualize the convergence behavior of all algorithms for case study-2, the convergence curves for SDeM and DDeM are illustrated in Fig. 15. From Fig. 15, it is observed that the convergence speed of the proposed CGBO algorithm is high compared to all other algorithms.

For case study-3, all the statistical data are listed in Table 22. Out of eight algorithms, the IMO algorithm holds the first position in terms of RT, followed by IPSO, PSO, CGBO, GBO, WOA, MPA, and EO. However, based on reliability (minimum STD) and Min values, the proposed CGBO holds the first position, followed by GBO, EO, MPA, WOA, IMO, IPSO, and PSO. To visualize the convergence

**TABLE 27.** SM55 - experimental data - different temperature at constant irradiance.

20°C		40°C		60°C	
V	I	V	I	V	I
0.00	3.45	0.00	3.47	0.00	3.50
11.84	3.45	10.83	3.47	10.18	3.48
12.51	3.45	11.89	3.45	10.51	3.48
13.03	3.44	12.13	3.45	10.78	3.48
13.49	3.43	12.62	3.44	11.24	3.47
14.00	3.43	13.16	3.43	11.73	3.45
14.46	3.42	13.52	3.42	12.16	3.43
14.98	3.41	14.03	3.40	12.54	3.41
15.60	3.39	14.49	3.36	13.14	3.36
16.02	3.36	15.10	3.31	13.71	3.30
16.64	3.32	15.49	3.27	14.19	3.23
17.09	3.28	16.04	3.19	14.79	3.11
17.60	3.21	16.58	3.08	15.17	3.01
18.11	3.12	17.07	2.94	15.70	2.85
18.54	3.00	17.53	2.77	16.20	2.62
19.04	2.82	18.01	2.52	16.75	2.30
19.48	2.60	18.51	2.15	17.28	1.88
20.11	2.12	19.01	1.73	17.77	1.45
20.56	1.72	19.53	1.25	18.26	0.98
21.03	1.28	20.02	0.72	18.76	0.43
21.50	0.79	20.50	0.16	19.10	0.00
22.02	0.17	20.61	0.00	-	-
22.16	0.00	-	-	-	-

behavior of all algorithms for case study - 3, the convergence curves for SDeM and DDeM are illustrated in Fig. 16. From Fig. 16, it is observed that the convergence speed of the proposed CGBO algorithm is high compared to all other algorithms.

For case study-4, all the statistical data are listed in Table 23. Out of eight algorithms, the IMO algorithm holds the first position in terms of RT, followed by PSO, IPSO, CGBO, GBO, WOA, MPA, and EO. However, based on reliability (minimum STD) and Min values, the proposed CGBO holds the first position, followed by GBO, EO, IMO, WOA, MPA, IPSO, and PSO. To visualize the convergence behavior of all algorithms for case study - 4, the convergence curves for testing conditions are illustrated in Fig. 17. From Fig. 17, it is observed that the convergence speed of the proposed CGBO algorithm is high compared to all other algorithms.

For case study-5, all the statistical data are listed in Table 24. Out of eight algorithms, the IMO algorithm holds the first position in terms of RT, followed by PSO, IPSO, CGBO, GBO, WOA, MPA, and EO. However, based on reliability (minimum STD) and Min values, the proposed CGBO holds the first position, followed by GBO, EO, MPA, IMO, WOA,

IPSO, and PSO. To visualize the convergence behavior of all algorithms for case study-5, the convergence curves for testing conditions are illustrated in Fig. 18. From Fig. 18, it is observed that the convergence speed of the proposed CGBO algorithm is high compared to all other algorithms.

As per the discussions, the proposed CGBO is superior to all other algorithms in identifying the best unknown parameters of the SDeM, DDeM, and PV module models. From the experimental findings, statistical analysis, and the performance comparison with other selected algorithms, it is concluded that the proposed CGBO algorithm can obtain the parameters of various PV models, including commercial modules. Based on the performance measures, including Min, Mean, Max, Mean, STD, RT, and rank, the effectiveness of the proposed CGBO algorithm is proved. Utilizing the chaotic map with the GBO algorithm benefits the CGBO algorithm to obtain excellent results due to the robust exploitation and exploration capabilities.

## V. CONCLUSION

This paper proposes a tent chaotic map-based GBO to improve the solution accuracy and speed up the convergence

rate of GBO while analyzing the photovoltaic model parameter identification optimization problem. CGBO, an improved variant of GBO, has a simple structure and is straightforward to execute. The efficiency of CGBO is thoroughly assessed by comparing it to the original GBO as well as the other six state-of-the-art algorithms. Experiments on various photovoltaic models under different environmental conditions show that the proposed CGBO can produce noticeably excellent performance than all other selected algorithms in terms of solution accuracy and convergence speed. More precisely, the proposed CGBO can achieve lower RMSE values, lower STD values, and quick convergence, thereby placing first among all other selected algorithms. In addition, the I-V characteristics generated by the proposed CGBO algorithm are very similar to the experimental samples. To summarize, the proposed CGBO algorithm extracts more precise and stable parameters with a quicker convergence speed, making it a promising solution to parameter estimation problems.

This study also introduces several opportunities for many other similar problems that require a highly competitive optimization technique. The suggested CGBO algorithm is not just an effective method for identifying the parameters of photovoltaic models, but it is also being developed for use and evaluation in identifying an effective solution to other engineering problems, such as information fusion, deep learning, machine learning, multipath routing, feature selection, image processing, image retrieval algorithm, social evolution modeling, wireless sensor networks, water pollution prediction, and disease diagnosis. In the future, the proposed CGBO algorithm is expected to apply in discrete optimization, industrial optimization problems, and it can also be applied to parameter optimization in renewable energy systems.

## ACKNOWLEDGMENT

The authors would like to thank the GMR Institute of Technology, Rajam, India, for providing the facility and allowing them to validate the performance of the system at the laboratory.

The opinions, findings, and conclusions or recommendations expressed in this material are those of the authors and do not necessarily reflect the views of the Science Foundation Ireland. For the purpose of Open Access the author has applied a CC BY public copyright license to any author accepted manuscript version arising from this submission.

## APPENDIX

See Tables 25–27.

## REFERENCES

- [1] M. Premkumar, K. Karthick, and R. Sowmya, “A review on solar PV based grid connected microinverter control schemes and topologies,” *Int. J. Renew. Energy Develop.*, vol. 7, no. 2, p. 171, Jul. 2018, doi: [10.14710/ijred.7.2.171-182](https://doi.org/10.14710/ijred.7.2.171-182).
- [2] N. Rajasekar, N. K. Kumar, and R. Venugopalan, “Bacterial foraging algorithm based solar PV parameter estimation,” *Sol. Energy*, vol. 97, pp. 255–265, Nov. 2013, doi: [10.1016/j.solener.2013.08.019](https://doi.org/10.1016/j.solener.2013.08.019).
- [3] D. Iqbal, T. Ahmad, I. Pervez, I. H. Malick, A. Sarwar, and M. Tariq, “Performance of PSO based variants in tracking optimal power in a solar PV based generation system under partial shading condition,” *Smart Sci.*, vol. 8, no. 1, pp. 1–13, Jan. 2020, doi: [10.1080/23080477.2019.1700067](https://doi.org/10.1080/23080477.2019.1700067).
- [4] M. Premkumar, R. Sowmya, P. Jangir, and J. S. V. S. Kumar, “A new and reliable objective functions for extracting the unknown parameters of solar photovoltaic cell using political optimizer algorithm,” in *Proc. Int. Conf. Data Analytics Bus. Ind., Way Towards Sustain. Economy (ICDABI)*, Oct. 2020, pp. 1–6, doi: [10.1109/ICDABI51230.2020.9325627](https://doi.org/10.1109/ICDABI51230.2020.9325627).
- [5] P. A. Kumari and P. Geethanjali, “Adaptive genetic algorithm based multi-objective optimization for photovoltaic cell design parameter extraction,” *Energy Procedia*, vol. 117, pp. 432–441, Jun. 2017, doi: [10.1016/j.egypro.2017.05.165](https://doi.org/10.1016/j.egypro.2017.05.165).
- [6] V. Khanna, B. K. Das, D. Bisht, and P. K. Singh, “A three diode model for industrial solar cells and estimation of solar cell parameters using PSO algorithm,” *Renew. Energy*, vol. 78, pp. 105–113, Jun. 2015, doi: [10.1016/j.renene.2014.12.072](https://doi.org/10.1016/j.renene.2014.12.072).
- [7] A. M. Humada, M. Hojabri, S. Mekhilef, and H. M. Hamada, “Solar cell parameters extraction based on single and double-diode models: A review,” *Renew. Sustain. Energy Rev.*, vol. 56, pp. 494–509, Apr. 2016, doi: [10.1016/j.rser.2015.11.051](https://doi.org/10.1016/j.rser.2015.11.051).
- [8] B. Romero, G. del Pozo, and B. Arredondo, “Exact analytical solution of a two diode circuit model for organic solar cells showing S-shape using lambert W-functions,” *Sol. Energy*, vol. 86, no. 10, pp. 3026–3029, Oct. 2012, doi: [10.1016/j.solener.2012.07.010](https://doi.org/10.1016/j.solener.2012.07.010).
- [9] P. Wolf and V. Benda, “Identification of PV solar cells and modules parameters by combining statistical and analytical methods,” *Sol. Energy*, vol. 93, pp. 151–157, Jul. 2013, doi: [10.1016/j.solener.2013.03.018](https://doi.org/10.1016/j.solener.2013.03.018).
- [10] E. I. Batzelis and S. A. Papathanassiou, “A method for the analytical extraction of the single-diode PV model parameters,” *IEEE Trans. Sustain. Energy*, vol. 7, no. 2, pp. 504–512, Apr. 2016, doi: [10.1109/TSTE.2015.2503435](https://doi.org/10.1109/TSTE.2015.2503435).
- [11] A. Farah and A. Belazi, “A novel chaotic Jaya algorithm for unconstrained numerical optimization,” *Nonlinear Dyn.*, vol. 93, no. 3, pp. 1451–1480, Aug. 2018, doi: [10.1007/s11071-018-4271-5](https://doi.org/10.1007/s11071-018-4271-5).
- [12] L. Sandrolini, M. Artioli, and U. Reggiani, “Numerical method for the extraction of photovoltaic module double-diode model parameters through cluster analysis,” *Appl. Energy*, vol. 87, no. 2, pp. 442–451, Feb. 2010, doi: [10.1016/j.apenergy.2009.07.022](https://doi.org/10.1016/j.apenergy.2009.07.022).
- [13] M. Premkumar, R. Sowmya, S. Umashankar, and J. Pradeep, “An effective solar photovoltaic module parameter estimation technique for single-diode model,” *IOP Conf. Ser., Mater. Sci. Eng.*, vol. 937, Oct. 2020, Art. no. 012014, doi: [10.1088/1757-899X/937/1/012014](https://doi.org/10.1088/1757-899X/937/1/012014).
- [14] A. M. Humada, S. Y. Darweesh, K. G. Mohammed, M. Kamil, S. F. Mohammed, N. K. Kasim, T. A. Tahseen, O. I. Awad, and S. Mekhilef, “Modeling of PV system and parameter extraction based on experimental data: Review and investigation,” *Sol. Energy*, vol. 199, pp. 742–760, Mar. 2020, doi: [10.1016/j.solener.2020.02.068](https://doi.org/10.1016/j.solener.2020.02.068).
- [15] A. R. Jordehi, “Parameter estimation of solar photovoltaic (PV) cells: A review,” *Renew. Sustain. Energy Rev.*, vol. 61, pp. 354–371, Aug. 2016, doi: [10.1016/j.rser.2016.03.049](https://doi.org/10.1016/j.rser.2016.03.049).
- [16] X. Wen-Bo, L. Wei-Qing, W. Hua-Ming, and Z. Hua-Ming, “Review of parameter extraction methods for single-diode model of solar cell,” *Acta Phys. Sinica*, vol. 67, no. 19, 2018, Art. no. 198801, doi: [10.7498/aps.67.20181024](https://doi.org/10.7498/aps.67.20181024).
- [17] V. J. Chin, Z. Salam, and K. Ishaque, “Cell modelling and model parameters estimation techniques for photovoltaic simulator application: A review,” *Appl. Energy*, vol. 154, pp. 500–519, Sep. 2015, doi: [10.1016/j.apenergy.2015.05.035](https://doi.org/10.1016/j.apenergy.2015.05.035).
- [18] R. Bendaoud, H. Amiry, M. Benhmida, B. Zohal, S. Yadir, S. Bounouar, C. Hajaj, E. Baghaz, and M. El Aydi, “New method for extracting physical parameters of PV generators combining an implemented genetic algorithm and the simulated annealing algorithm,” *Sol. Energy*, vol. 194, pp. 239–247, Dec. 2019, doi: [10.1016/j.solener.2019.10.040](https://doi.org/10.1016/j.solener.2019.10.040).
- [19] M. Zagrouba, A. Sellami, M. Bouaicha, and M. Ksouri, “Identification of PV solar cells and modules parameters using the genetic algorithms: Application to maximum power extraction,” *Sol. Energy*, vol. 84, no. 5, pp. 860–866, May 2010, doi: [10.1016/j.solener.2010.02.012](https://doi.org/10.1016/j.solener.2010.02.012).
- [20] S. Bana and R. P. Saini, “Identification of unknown parameters of a single diode photovoltaic model using particle swarm optimization with binary constraints,” *Renew. Energy*, vol. 101, pp. 1299–1310, Feb. 2017, doi: [10.1016/j.renene.2016.10.010](https://doi.org/10.1016/j.renene.2016.10.010).

- [21] J. Liang, S. Ge, B. Qu, K. Yu, F. Liu, H. Yang, P. Wei, and Z. Li, "Classified perturbation mutation based particle swarm optimization algorithm for parameters extraction of photovoltaic models," *Energy Convers. Manage.*, vol. 203, Jan. 2020, Art. no. 112138, doi: [10.1016/j.enconman.2019.112138](https://doi.org/10.1016/j.enconman.2019.112138).
- [22] T. Wei, F. Yu, G. Huang, and C. Xu, "A particle-swarm-optimization-based parameter extraction routine for three-diode lumped parameter model of organic solar cells," *IEEE Electron Device Lett.*, vol. 40, no. 9, pp. 1511–1514, Sep. 2019, doi: [10.1109/LED.2019.2926315](https://doi.org/10.1109/LED.2019.2926315).
- [23] A. R. Jordehi, "Enhanced leader particle swarm optimisation (ELPSO): An efficient algorithm for parameter estimation of photovoltaic (PV) cells and modules," *Sol. Energy*, vol. 159, pp. 78–87, Jan. 2018, doi: [10.1016/j.solener.2017.10.063](https://doi.org/10.1016/j.solener.2017.10.063).
- [24] X. Lin and Y. Wu, "Parameters identification of photovoltaic models using niche-based particle swarm optimization in parallel computing architecture," *Energy*, vol. 196, Apr. 2020, Art. no. 117054, doi: [10.1016/j.energy.2020.117054](https://doi.org/10.1016/j.energy.2020.117054).
- [25] P. P. Biswas, P. N. Suganthan, G. Wu, and G. A. J. Amaralunga, "Parameter estimation of solar cells using datasheet information with the application of an adaptive differential evolution algorithm," *Renew. Energy*, vol. 132, pp. 425–438, Mar. 2019, doi: [10.1016/j.renene.2018.07.152](https://doi.org/10.1016/j.renene.2018.07.152).
- [26] H. M. Ridha, H. Hizam, C. Gomes, A. A. Heidari, H. Chen, M. Ahmadipour, D. H. Muhsen, and M. Alghrairi, "Parameters extraction of three diode photovoltaic models using boosted LSHADE algorithm and Newton Raphson method," *Energy*, vol. 224, Jun. 2021, Art. no. 120136, doi: [10.1016/j.energy.2021.120136](https://doi.org/10.1016/j.energy.2021.120136).
- [27] Z. Hu, W. Gong, and S. Li, "Reinforcement learning-based differential evolution for parameters extraction of photovoltaic models," *Energy Rep.*, vol. 7, pp. 916–928, Nov. 2021, doi: [10.1016/j.egyr.2021.01.096](https://doi.org/10.1016/j.egyr.2021.01.096).
- [28] X. Yang, W. Gong, and L. Wang, "Comparative study on parameter extraction of photovoltaic models via differential evolution," *Energy Convers. Manage.*, vol. 201, Dec. 2019, Art. no. 112113, doi: [10.1016/j.enconman.2019.112113](https://doi.org/10.1016/j.enconman.2019.112113).
- [29] K. Ishaque, Z. Salam, S. Mekhilef, and A. Shamsudin, "Parameter extraction of solar photovoltaic modules using penalty-based differential evolution," *Appl. Energy*, vol. 99, pp. 297–308, Nov. 2012, doi: [10.1016/j.apenergy.2012.05.017](https://doi.org/10.1016/j.apenergy.2012.05.017).
- [30] M. H. Qais, H. M. Hasaniem, and S. Alghuwainem, "Identification of electrical parameters for three-diode photovoltaic model using analytical and sunflower optimization algorithm," *Appl. Energy*, vol. 250, pp. 109–117, Sep. 2019, doi: [10.1016/j.apenergy.2019.05.013](https://doi.org/10.1016/j.apenergy.2019.05.013).
- [31] A. Saxena, A. Sharma, and S. Shekhawat, "Parameter extraction of solar cell using intelligent grey wolf optimizer," *Evol. Intell.*, pp. 1–17, Oct. 2020, doi: [10.1007/s12065-020-00499-1](https://doi.org/10.1007/s12065-020-00499-1).
- [32] G. Xiong, J. Zhang, D. Shi, and Y. He, "Parameter extraction of solar photovoltaic models using an improved whale optimization algorithm," *Energy Convers. Manage.*, vol. 174, pp. 388–405, Oct. 2018, doi: [10.1016/j.enconman.2018.08.053](https://doi.org/10.1016/j.enconman.2018.08.053).
- [33] M. H. Qais, H. M. Hasaniem, and S. Alghuwainem, "Parameters extraction of three-diode photovoltaic model using computation and Harris Hawks optimization," *Energy*, vol. 195, Mar. 2020, Art. no. 117040, doi: [10.1016/j.energy.2020.117040](https://doi.org/10.1016/j.energy.2020.117040).
- [34] R. Abbassi, A. Abbassi, A. A. Heidari, and S. Mirjalili, "An efficient salp swarm-inspired algorithm for parameters identification of photovoltaic cell models," *Energy Convers. Manage.*, vol. 179, pp. 362–372, Jan. 2019, doi: [10.1016/j.enconman.2018.10.069](https://doi.org/10.1016/j.enconman.2018.10.069).
- [35] M. Premkumar, P. Jangir, R. Sowmya, R. M. Elavarasan, and B. S. Kumar, "Enhanced chaotic JAYA algorithm for parameter estimation of photovoltaic cell/modules," *ISA Trans.*, pp. 1–28, Jan. 2021, doi: [10.1016/j.isatra.2021.01.045](https://doi.org/10.1016/j.isatra.2021.01.045).
- [36] K. Yu, J. J. Liang, B. Y. Qu, Z. Cheng, and H. Wang, "Multiple learning backtracking search algorithm for estimating parameters of photovoltaic models," *Appl. Energy*, vol. 226, pp. 408–422, Sep. 2018, doi: [10.1016/j.apenergy.2018.06.010](https://doi.org/10.1016/j.apenergy.2018.06.010).
- [37] A. A. Z. Diab, H. M. Sultan, T. D. Do, O. M. Kamel, and M. A. Mossa, "Coyote optimization algorithm for parameters estimation of various models of solar cells and PV modules," *IEEE Access*, vol. 8, pp. 111102–111140, 2020, doi: [10.1109/ACCESS.2020.3000770](https://doi.org/10.1109/ACCESS.2020.3000770).
- [38] S. Li, W. Gong, X. Yan, C. Hu, D. Bai, L. Wang, and L. Gao, "Parameter extraction of photovoltaic models using an improved teaching-learning-based optimization," *Energy Convers. Manage.*, vol. 186, pp. 293–305, Apr. 2019, doi: [10.1016/j.enconman.2019.02.048](https://doi.org/10.1016/j.enconman.2019.02.048).
- [39] Z. Liao, Z. Chen, and S. Li, "Parameters extraction of photovoltaic models using triple-phase teaching-learning-based optimization," *IEEE Access*, vol. 8, pp. 69937–69952, 2020, doi: [10.1109/ACCESS.2020.2984728](https://doi.org/10.1109/ACCESS.2020.2984728).
- [40] B. Mandal and P. Kumar Roy, "Multi-objective optimal power flow using quasi-oppositional teaching learning based optimization," *Appl. Soft Comput.*, vol. 21, pp. 590–606, Aug. 2014, doi: [10.1016/j.asoc.2014.04.010](https://doi.org/10.1016/j.asoc.2014.04.010).
- [41] K. Yu, X. Chen, X. Wang, and Z. Wang, "Parameters identification of photovoltaic models using self-adaptive teaching-learning-based optimization," *Energy Convers. Manage.*, vol. 145, pp. 233–246, Aug. 2017, doi: [10.1016/j.enconman.2017.04.054](https://doi.org/10.1016/j.enconman.2017.04.054).
- [42] X. Chen, K. Yu, W. Du, W. Zhao, and G. Liu, "Parameters identification of solar cell models using generalized oppositional teaching learning based optimization," *Energy*, vol. 99, pp. 170–180, Mar. 2016, doi: [10.1016/j.energy.2016.01.052](https://doi.org/10.1016/j.energy.2016.01.052).
- [43] Y. Liu, A. A. Heidari, X. Ye, C. Chi, X. Zhao, C. Ma, H. Turabieh, H. Chen, and R. Le, "Evolutionary shuffled frog leaping with memory pool for parameter optimization," *Energy Rep.*, vol. 7, pp. 584–606, Nov. 2021, doi: [10.1016/j.egyr.2021.01.001](https://doi.org/10.1016/j.egyr.2021.01.001).
- [44] C. Kumar, T. D. Raj, M. Premkumar, and T. D. Raj, "A new stochastic slime mould optimization algorithm for the estimation of solar photovoltaic cell parameters," *Optik*, vol. 223, Dec. 2020, Art. no. 165277, doi: [10.1016/j.ijleo.2020.165277](https://doi.org/10.1016/j.ijleo.2020.165277).
- [45] A. A. El-Fergany, "Parameters identification of PV model using improved slime mould optimizer and lambert W-function," *Energy Rep.*, vol. 7, pp. 875–887, Nov. 2021, doi: [10.1016/j.egyr.2021.01.093](https://doi.org/10.1016/j.egyr.2021.01.093).
- [46] H. M. Ridha, "Parameters extraction of single and double diodes photovoltaic models using Marine Predators Algorithm and Lambert W function," *Sol. Energy*, vol. 209, pp. 674–693, Oct. 2020, doi: [10.1016/j.solener.2020.09.047](https://doi.org/10.1016/j.solener.2020.09.047).
- [47] M. Abdel-Basset, R. Mohamed, S. Mirjalili, R. K. Chakrabortty, and M. J. Ryan, "Solar photovoltaic parameter estimation using an improved equilibrium optimizer," *Sol. Energy*, vol. 209, pp. 694–708, Oct. 2020, doi: [10.1016/j.solener.2020.09.032](https://doi.org/10.1016/j.solener.2020.09.032).
- [48] B. Javidy, A. Hatamlou, and S. Mirjalili, "Ions motion algorithm for solving optimization problems," *Appl. Soft Comput.*, vol. 32, pp. 72–79, Jul. 2015, doi: [10.1016/j.asoc.2015.03.035](https://doi.org/10.1016/j.asoc.2015.03.035).
- [49] S. Kumar, A. Singh, and A. Dhar, "Parameter extraction using global particle swarm optimization approach and the influence of polymer processing temperature on the solar cell parameters," *AIP Adv.*, vol. 7, no. 8, p. 85117, 2017, doi: [10.1063/1.4993999](https://doi.org/10.1063/1.4993999).
- [50] A. M. Shaheen, A. R. Ginidi, R. A. El-Sehiemy, and S. S. M. Ghoneim, "A forensic-based investigation algorithm for parameter extraction of solar cell models," *IEEE Access*, vol. 9, pp. 1–20, 2021, doi: [10.1109/ACCESS.2020.3046536](https://doi.org/10.1109/ACCESS.2020.3046536).
- [51] T. Huang, C. Zhang, H. Ouyang, G. Luo, S. Li, and D. Zou, "Parameter identification for photovoltaic models using an improved learning search algorithm," *IEEE Access*, vol. 8, pp. 116292–116309, 2020, doi: [10.1109/ACCESS.2020.3003814](https://doi.org/10.1109/ACCESS.2020.3003814).
- [52] W. Long, S. Cai, J. Jiao, M. Xu, and T. Wu, "A new hybrid algorithm based on grey wolf optimizer and cuckoo search for parameter extraction of solar photovoltaic models," *Energy Convers. Manage.*, vol. 203, Jan. 2020, Art. no. 112243, doi: [10.1016/j.enconman.2019.112243](https://doi.org/10.1016/j.enconman.2019.112243).
- [53] A. M. Beigi and A. Maroosi, "Parameter identification for solar cells and module using a hybrid firefly and pattern search algorithms," *Sol. Energy*, vol. 171, pp. 435–446, Sep. 2018, doi: [10.1016/j.solener.2018.06.092](https://doi.org/10.1016/j.solener.2018.06.092).
- [54] M. Premkumar, R. Sowmya, S. Umashankar, and P. Jangir, "Extraction of uncertain parameters of single-diode photovoltaic module using hybrid particle swarm optimization and grey wolf optimization algorithm," *Mater. Today, Proc.*, pp. 1–7, Oct. 2020, doi: [10.1016/j.matpr.2020.08.784](https://doi.org/10.1016/j.matpr.2020.08.784).
- [55] D. H. Wolpert and W. G. Macready, "No free lunch theorems for optimization," *IEEE Trans. Evol. Comput.*, vol. 1, no. 1, pp. 67–82, Apr. 1997.
- [56] A. Senouci, H. Bouhedjoud, K. Tourche, and A. Boukabou, "FPGA based hardware and device-independent implementation of chaotic generators," *AEU-Int. J. Electron. Commun.*, vol. 82, pp. 211–220, Dec. 2017, doi: [10.1016/j.aeue.2017.08.011](https://doi.org/10.1016/j.aeue.2017.08.011).
- [57] D. Oliva, A. A. Ewees, M. A. E. Aziz, A. E. Hassannien, and M. Peréz-Cisneros, "A chaotic improved artificial bee colony for parameter estimation of photovoltaic cells," *Energies*, vol. 10, no. 7, p. 865, Jun. 2017, doi: [10.3390/en10070865](https://doi.org/10.3390/en10070865).
- [58] X. Jian and Z. Weng, "A logistic chaotic JAYA algorithm for parameters identification of photovoltaic cell and module models," *Optik*, vol. 203, Feb. 2020, Art. no. 164041, doi: [10.1016/j.ijleo.2019.164041](https://doi.org/10.1016/j.ijleo.2019.164041).

- [59] D. Yousri, S. B. Thanikanti, D. Allam, V. K. Ramachandaramurthy, and M. B. Eteiba, "Fractional chaotic ensemble particle swarm optimizer for identifying the single, double, and three diode photovoltaic models' parameters," *Energy*, vol. 195, Mar. 2020, Art. no. 116979, doi: [10.1016/j.energy.2020.116979](https://doi.org/10.1016/j.energy.2020.116979).
- [60] D. Yousri, D. Allam, M. B. Eteiba, and P. N. Suganthan, "Static and dynamic photovoltaic models' parameters identification using chaotic heterogeneous comprehensive learning particle swarm optimizer variants," *Energy Convers. Manage.*, vol. 182, pp. 546–563, Feb. 2019, doi: [10.1016/j.enconman.2018.12.022](https://doi.org/10.1016/j.enconman.2018.12.022).
- [61] D. Oliva, M. A. El Aziz, and A. E. Hassanien, "Parameter estimation of photovoltaic cells using an improved chaotic whale optimization algorithm," *Appl. Energy*, vol. 200, pp. 141–154, Aug. 2017, doi: [10.1016/j.apenergy.2017.05.029](https://doi.org/10.1016/j.apenergy.2017.05.029).
- [62] H. Chen, S. Jiao, M. Wang, A. A. Heidari, and X. Zhao, "Parameters identification of photovoltaic cells and modules using diversification-enriched Harris Hawks optimization with chaotic drifts," *J. Cleaner Prod.*, vol. 244, Jan. 2020, Art. no. 118778, doi: [10.1016/j.jclepro.2019.118778](https://doi.org/10.1016/j.jclepro.2019.118778).
- [63] Y. Liu, G. Chong, A. A. Heidari, H. Chen, G. Liang, X. Ye, Z. Cai, and M. Wang, "Horizontal and vertical crossover of Harris hawk optimizer with Nelder-Mead simplex for parameter estimation of photovoltaic models," *Energy Convers. Manage.*, vol. 223, Nov. 2020, Art. no. 113211, doi: [10.1016/j.enconman.2020.113211](https://doi.org/10.1016/j.enconman.2020.113211).
- [64] I. Ahmadianfar, O. Bozorg-Haddad, and X. Chu, "Gradient-based optimizer: A new Metaheuristic optimization algorithm," *Inf. Sci.*, vol. 540, pp. 131–159, Nov. 2020, doi: [10.1016/j.ins.2020.06.037](https://doi.org/10.1016/j.ins.2020.06.037).
- [65] A. A. K. Ismaeel, E. H. Houssein, D. Oliva, and M. Said, "Gradient-based optimizer for parameter extraction in photovoltaic models," *IEEE Access*, vol. 9, pp. 13403–13416, 2021, doi: [10.1109/ACCESS.2021.3052153](https://doi.org/10.1109/ACCESS.2021.3052153).
- [66] M. Premkumar, C. Kumar, and R. Sowmya, "Mathematical modelling of solar photovoltaic cell/panel/array based on the physical parameters from the manufacturer's datasheet," *Int. J. Renew. Energy Develop.*, vol. 9, no. 1, pp. 7–22, Feb. 2020, doi: [10.14710/ijred.9.1.7-22](https://doi.org/10.14710/ijred.9.1.7-22).
- [67] M. Premkumar, U. Subramaniam, T. S. Babu, R. M. Elavarasan, and L. Mihet-Popa, "Evaluation of mathematical model to characterize the performance of conventional and hybrid PV array topologies under static and dynamic shading patterns," *Energies*, vol. 13, no. 12, p. 3216, Jun. 2020, doi: [10.3390/en13123216](https://doi.org/10.3390/en13123216).
- [68] M. Premkumar and R. Sowmya, "An effective maximum power point tracker for partially shaded solar photovoltaic systems," *Energy Rep.*, vol. 5, pp. 1445–1462, Nov. 2019, doi: [10.1016/j.egyr.2019.10.006](https://doi.org/10.1016/j.egyr.2019.10.006).
- [69] M. Premkumar, T. S. Babu, S. Umashankar, and R. Sowmya, "A new metaphor-less algorithms for the photovoltaic cell parameter estimation," *Optik*, vol. 208, Apr. 2020, Art. no. 164559, doi: [10.1016/j.ijleo.2020.164559](https://doi.org/10.1016/j.ijleo.2020.164559).



**PRADEEP JANGIR** is currently the Co-Director of the Zero Lab Optimization, Gujarat and Power Engineer, RVPN, Jaipur, India. He is internationally recognized for his advances in Swarm Intelligence and Optimization. He has published over 76 publications with over 1000 citations and an H-index of 15. His research interests include many-objective, robust optimization, power system engineering optimization, multi-objective optimization, swarm intelligence, evolutionary neural networks. He is working on the application of multi-objective, many-objective, and robust meta-heuristic optimization techniques as well.



**C. RAMAKRISHNAN** (Member, IEEE) received the B.E. degree in electrical and electronics engineering from the Karunya Institute of Technology, Coimbatore, in 1998, the M.E. degree in power electronics and drives from the PSG College of Technology, Coimbatore, in 2003, and the Ph.D. degree in power electronics and power quality from Anna University, Chennai, in 2017. He is currently working as an Associate Professor and the Head of the Department of Electrical and Electronics Engineering, SNS College of Technology, Coimbatore. He has published research papers in both national and international reputed journals and presented papers in national and international conferences. His research interests include power converters, distribution generation, power quality, and smart grids. He is also a Life Member of ISTE and IE.



**M. PREMKUMAR** (Member, IEEE) was born in Coimbatore, India. He received the B.E. degree in electrical and electronics engineering from the Sri Ramakrishna Institute of Technology, Coimbatore, in 2004, the M.E. degree in applied electronics from the Anna University of Technology, Coimbatore, in 2010, and the Ph.D. degree from Anna University, Chennai, India, in 2019. He is currently working as an Assistant Professor with the GMR Institute of Technology, Rajam, India. He has more than 12 years of teaching experience, and he has published more than 65 technical articles in various national/international peer-reviewed journals, such as IEEE, Elsevier, Springer, and so on, over 300 citations and an H-index of 11. He has published/granted four patents accepted and approved by IPR, India, and IPR, Australia. He is also serving as an editor/reviewer for leading journals, such as IEEE, IET, Wiley, Taylor & Francis, and Springer. His current research interests include optimization techniques, including single-, multi-, and many-objectives, solar PV microinverter, solar PV parameter extraction, modern solar PVMPPTs (optimization technique based), PV array faults, and non-isolated/isolated dc-dc converters for PV systems. He is also a member of various professional bodies, such as IEEE, ISTE, and IAENG.

with a high impact factor. She also published three patents in cutting-edge technologies accepted by Intellectual Property Rights, India. She has been invited as a resource person for workshops, seminars, and faculty development programs in various engineering colleges, universities around India and Abroad. She has visited foreign universities, such as France, Singapore, and Malaysia. She has guided many projects in UG, PG, and Ph.D. levels. Her research interests include artificial intelligence, machine learning, data science, the IoT, big data analytics, language computing, and cloud security. She is also a member of many professional bodies, such as IEEE, ISTE, ACEEE, CSTA, IAENG, and ISRD. She is also an editor and a reviewer for many international books and journals. She received the "Outstanding Contribution in Reviewing" Award from *Indian Heart Journal* (Elsevier).



**HASSAN HAES ALHEOU** (Senior Member, IEEE) received the B.Sc. degree (Hons.) from Tishreen University, Lattakia, Syria, in 2011, and the M.Sc. degree (Hons.) from the Isfahan University of Technology (IUT), Isfahan, Iran, in 2016, all in electrical power engineering, power systems. Since 2016, he has been started his Ph.D. Research at IUT. He is currently with the School of Electrical and Electronic Engineering, University College Dublin, Dublin, Ireland. He is also a Faculty Member with Tishreen University. He is included in the 2018 Publons list of the top 1% best reviewer and researchers in the field of engineering in the world. He has published more than 130 research papers in high-quality peer-reviewed journals and international conferences. He has also performed more than 600 reviews for high prestigious journals, including IEEE TRANSACTIONS ON INDUSTRIAL INFORMATICS, IEEE TRANSACTIONS ON INDUSTRIAL ELECTRONICS, *Energy Conversion and Management*, *Applied Energy*, and *International Journal of Electrical Power & Energy Systems*. He has participated in more than 15 industrial projects. His research interests include power systems, power system dynamics, power system operation and control, dynamic state estimation, frequency control, smart grids, micro-grids, demand response, and load shedding. He was a recipient of the Outstanding Reviewer Award from many journals, e.g., *Energy Conversion and Management (ECM)*, *ISA Transactions*, and *Applied Energy*. He was also a recipient of the best young researcher in the Arab Student Forum Creative among 61 researchers from 16 countries at Alexandria University, Egypt, in 2011.



**B. SANTHOSH KUMAR** (Senior Member, IEEE) was born in Ooty, India, in March 1980. He received the B.E. degree in computer science and engineering from Bharathiar University, Coimbatore, the M.E. degree in computer science and engineering from Anna University, Tiruchirappalli, and the Ph.D. degree in information and communication engineering from Anna University, Chennai. He has more than 16 years of experience and is currently working as a Professor with the Department of Computer Science and Engineering, Guru Nanak Institute of Technology, Hyderabad. He has more than 80 publications in a total of which are 35 journal publications and 45 are conference publications. He has delivered 15 guest lectures and keynote speeches on various occasions. His research interests include data science, machine learning, blockchain technology, data mining, and web mining. He is also an ACM Distinguished Speaker. He received 11 awards from various professional bodies. He is also serving as a Reviewer for reputed journals globally, such as IEEE TRANSACTIONS, IEEE ACCESS, *ACM Transactions*, *Complex & Intelligence Systems*, and *Computer Communications*, and various international conferences organized by ASDF, IEEE, and Springer.

• • •